

Journal Pre-proof



Chromosome-level Genome Reveals the Origin of Neo-Y Chromosome in the Male Barred knifejaw *Oplegnathus fasciatus*

Yongshuang Xiao, Zhizhong Xiao, Daoyuan Ma, Chenxi Zhao, Lin Liu, Hao Wu, Wenchao Nie, Shijun Xiao, Jing Liu, Jun Li, Angel Herrera-Ulloa

PII: S2589-0042(20)30223-6

DOI: <https://doi.org/10.1016/j.isci.2020.101039>

Reference: ISCI 101039

To appear in: *ISCIENCE*

Received Date: 11 December 2019

Revised Date: 5 March 2020

Accepted Date: 1 April 2020

Please cite this article as: Xiao, Y., Xiao, Z., Ma, D., Zhao, C., Liu, L., Wu, H., Nie, W., Xiao, S., Liu, J., Li, J., Herrera-Ulloa, A., Chromosome-level Genome Reveals the Origin of Neo-Y Chromosome in the Male Barred knifejaw *Oplegnathus fasciatus*, *ISCIENCE* (2020), doi: <https://doi.org/10.1016/j.isci.2020.101039>.

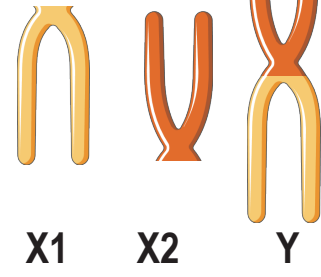
This is a PDF file of an article that has undergone enhancements after acceptance, such as the addition of a cover page and metadata, and formatting for readability, but it is not yet the definitive version of record. This version will undergo additional copyediting, typesetting and review before it is published in its final form, but we are providing this version to give early visibility of the article. Please note that, during the production process, errors may be discovered which could affect the content, and all legal disclaimers that apply to the journal pertain.

© 2020 The Author(s).



Barred knifejaw
Oplegnathus fasciatus

Male

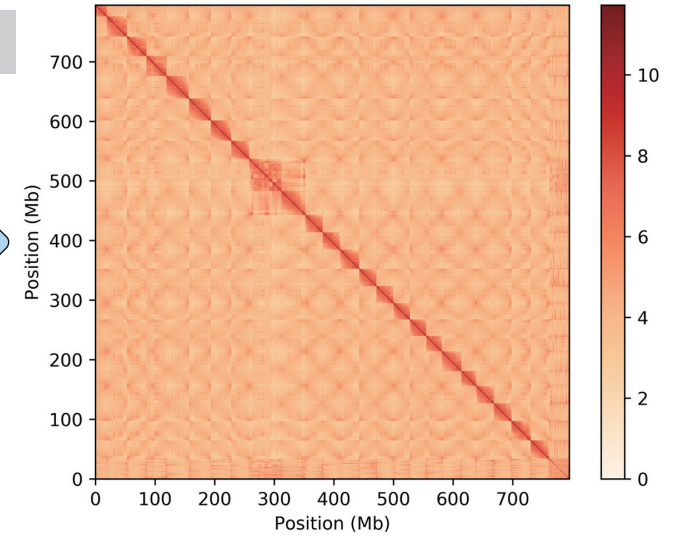
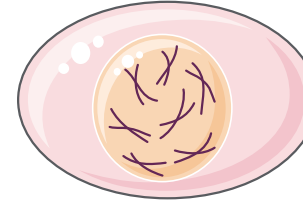


X1

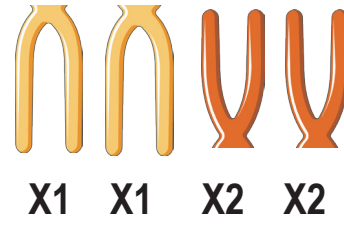
X2

Y

2n = 47



Female



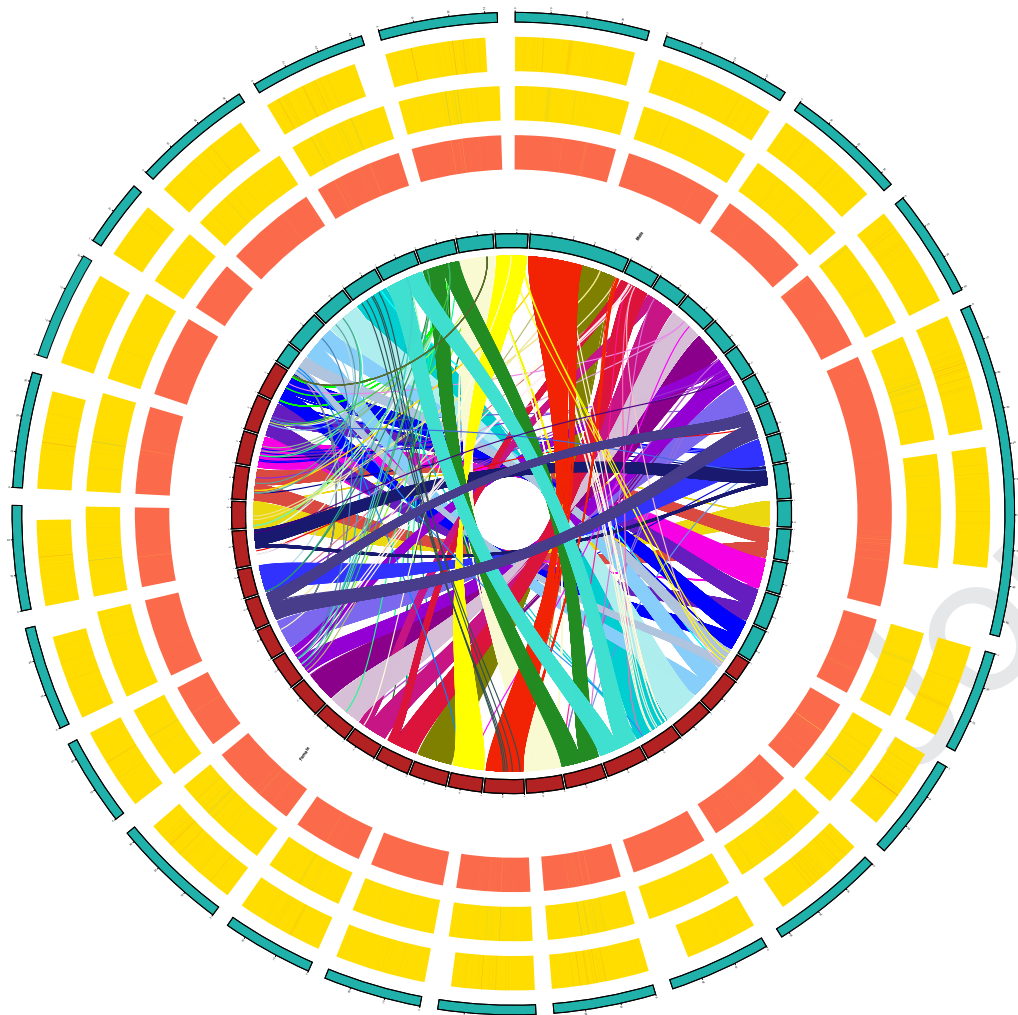
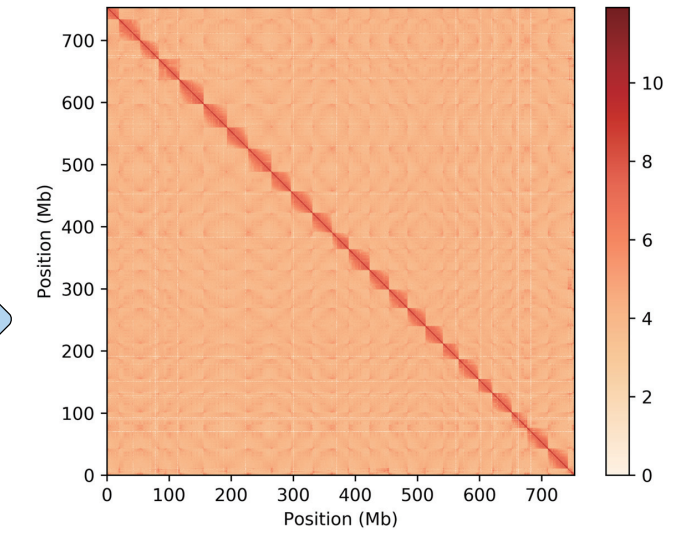
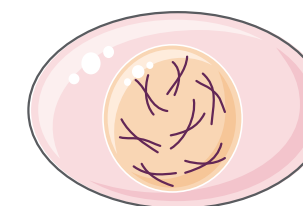
X1

X1

X2

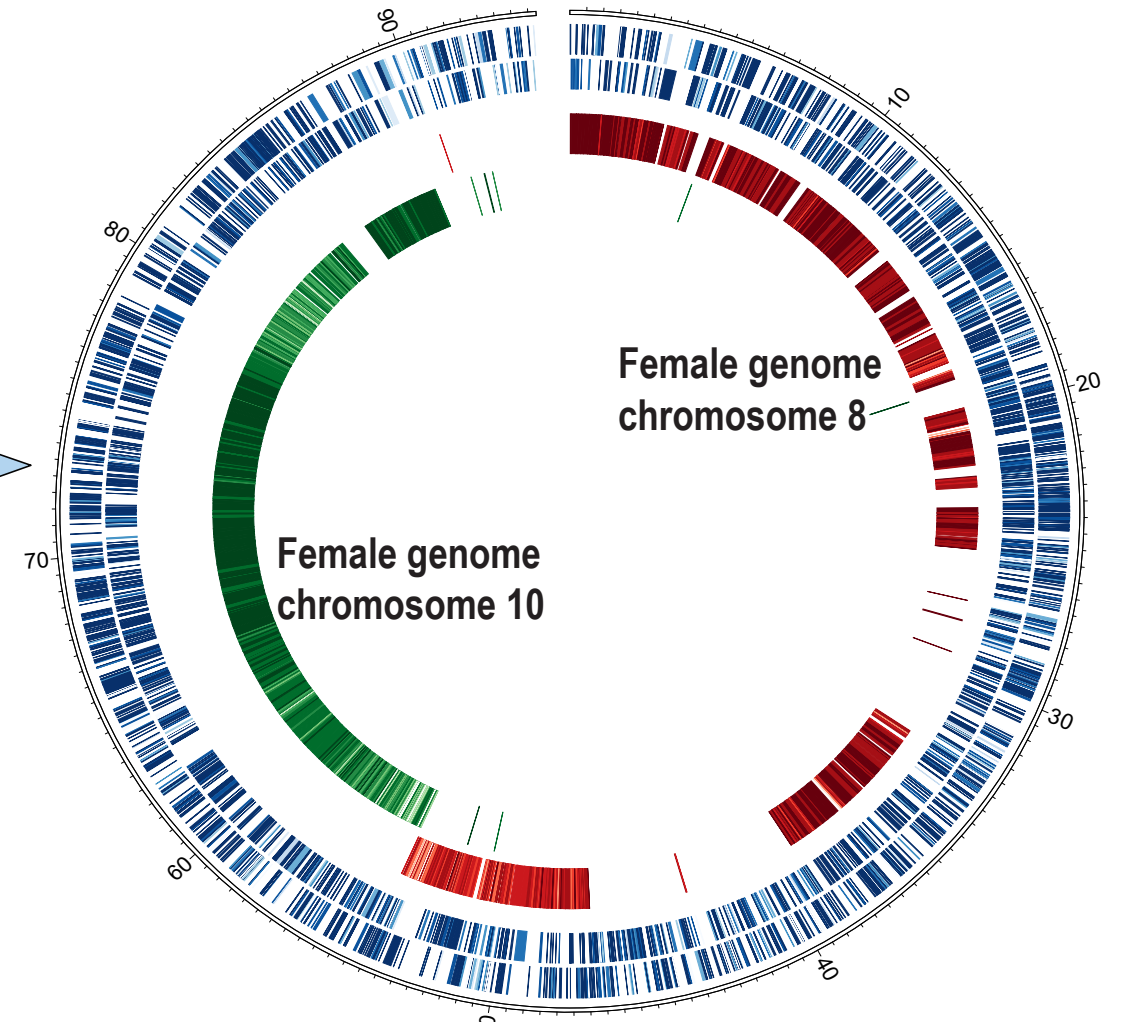
X2

2n = 48



Male genome with 23 chromosomes

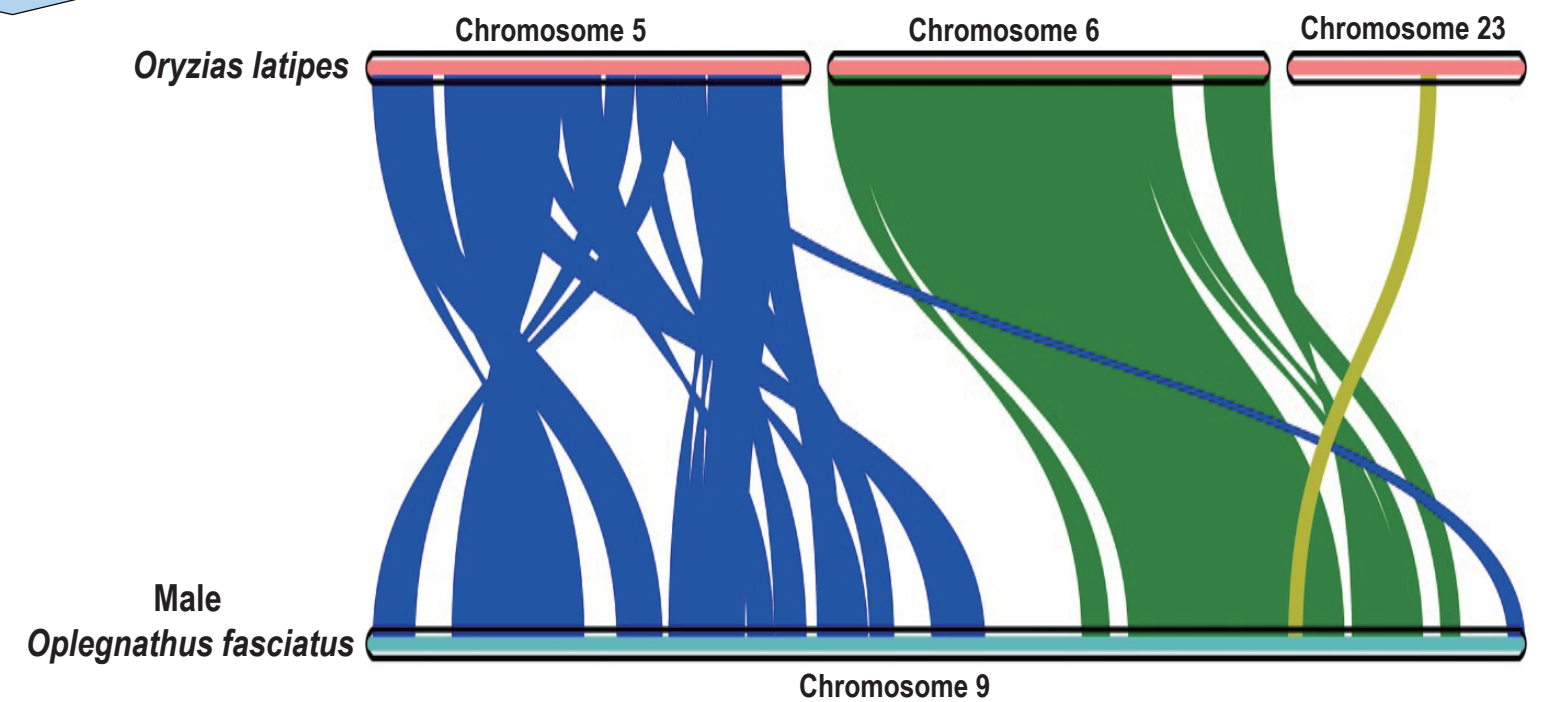
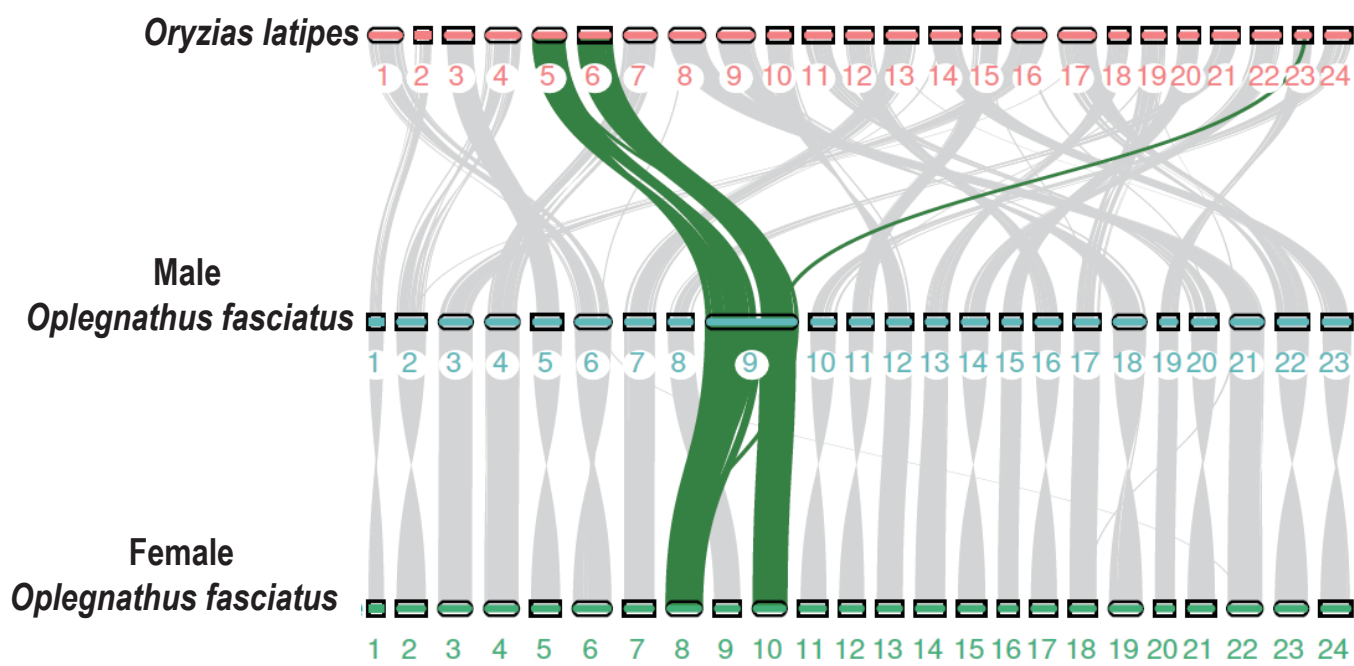
Male genome chromosome 9



Female genome chromosome 8

Female genome chromosome 10

Male genome chromosome 9



1 **Chromosome-level Genome Reveals the Origin of Neo-Y**
2 **Chromosome in the Male Barred knifejaw *Oplegnathus***
3 ***fasciatus***

4 Yongshuang Xiao^{1,2,8}, Zhizhong Xiao^{1,2,8}, Daoyuan Ma^{1,2}, Chenxi Zhao³, Lin Liu⁴,
5 Hao Wu⁴, Wenchao Nie⁴, Shijun Xiao^{5, 6*}, Jing Liu^{1, 2*} and Jun Li^{1, 2, 9*}, Angel
6 Herrera-Ulloa⁷

7 ¹Center for Ocean Mega-Science, The Key Laboratory of Experimental Marine
8 Biology, Institute of Oceanology, Chinese Academy of Sciences, Qingdao, China

9 ²Laboratory for Marine Biology and Biotechnology, Qingdao National Laboratory for
10 Marine Science and Technology, Qingdao, China

11 ³BGI Education Center, University of Chinese Academy of Sciences, Shenzhen,
12 China,

13 ⁴Wuhan FraserGen Bioinformatics Co., Ltd. East Lake High-Tech Zone, Wuhan,
14 China.

15 ⁵College of Plant Protection, Jilin Agriculture University, Changchun, Jilin, China

16 ⁶School of Computer Science and Technology, Wuhan University of Technology,
17 Wuhan, China

18 ⁷Escuela de Ciencias Biológicas, Universidad Nacional, San José, Costa Rica

19 ⁸These authors contributed equally

20 ⁹Lead Contact

21 *Correspondence:

22 shijun_xiao@163.com (S.J.X.), jliu@qdio.ac.cn (J.L.), junli@qdio.ac.cn (J.L.)

23
24 **SUMMARY**

25 The Barred knifejaw, *Oplegnathus fasciatus*, is characterized by an X₁X₂Y system
26 with a neo-Y chromosome for males. Here, a chromosome-level genome was
27 assembled to investigate the origin of neo-Y chromosome to the male *O. fasciatus*.

28 Twenty-three chromosomes corresponding to the male karyotypes were scaffolded to
29 762 Mb genome with a contig N50 length of 2.18 Mb. A large neo-Y chromosome

30 (*Ch9*) in the male *O. fasciatus* genome was also assembled and exhibited high identity
31 to those of the female chromosomes *Ch8* and *Ch10*. Chromosome rearrangements
32 events were detected in the neo-chromosome *Ch9*. Our results suggested that a centric
33 fusion of acrocentric chromosomes *Ch8* and *Ch10* should be responsible for the
34 formation of the X_1X_2Y system. The high-quality genome will not only provide a
35 solid foundation for further sex-determining mechanism research in the X_1X_2Y
36 system, but also facilitate the artificial breeding aiming to improve the yield and
37 disease resistance for *Oplegnathus*.

38

39 INTRODUCTION

40 The barred knifejaw (*Oplegnathus fasciatus*) (FishBase ID: 1709; NCBI Taxonomy
41 ID: 163134) (Temminck & Schlegel, 1844), a member of the Oplegnathidae family of
42 the Centrarchiformes, is a commercially important rocky reef fish native to East Asia.
43 *O. fasciatus* has become an important fishery resource in offshore cage aquaculture
44 and fish stocking for marine ranching in China, Japan and Korea (Schembri et al.,
45 2010; Xiao et al., 2016; Xiao et al., 2019). This fish is also a valuable species for
46 sashimi and recreational fishing, and its the ex-factory price has reached up to 30
47 dollars per kilogram in China (Xiao et al., 2015; Park et al., 2018). It has been
48 reported that the male of *O. fasciatus* has $2n=47$ chromosomes ($1m + 2m/sm + 44t$),
49 while females possess $2n=48$ chromosomes ($2m/sm + 46t$) (Xu et al., 2012; Xu et al.,
50 2019). Similar chromosome karyotypes have also been reported in male and female
51 individuals of *O. punctatus* (Xue et al., 2016; Xu et al., 2019). A large metacentric Y
52 chromosome was found in male individuals of *O. fasciatus* and *O. punctatus* based on
53 karyotypes and microsatellite DNA motif analyses, and it was suggested that the
54 sex-determining types of *O. fasciatus* and *O. punctatus* should belong to the multiple
55 $X_1X_1X_2X_2/X_1X_2Y$ sexual system (Xu et al. 2012; Xue et al. 2016; Xu et al., 2019).
56 Sexual dimorphism in growth has been detected in *O. fasciatus*, with male fish
57 exhibiting faster growth than females, possibly due to the sex chromosome system in
58 *Oplegnathus* (Xiao et al., 2015). *O. fasciatus* is vulnerable to viruses (e.g., iridovirus)
59 due to inbreeding in aquaculture industry (Li et al., 2011; Zhang et al. 2014). Its high

60 aquaculture value, multiple $X_1X_1X_2X_2/X_1X_2Y$ sex chromosome system, and
61 susceptibility to widespread biotic diseases have led to increasing research interests in
62 *O. fasciatus*. Although the previous reports provided a preliminary description of the
63 multiple sex chromosome system, the exact origin and molecular composition of the
64 large metacentric Y chromosome of the X_1X_2Y system at the genomic level remain
65 unclear.

66 Approximately 37 cases of multiple sex chromosomes with $X_1X_1X_2X_2/X_1X_2Y$ system
67 have been reported across the teleost phylogeny (Sember et al., 2015; Bitencourt et al.,
68 2016; Zhang et al., 2018; Krysanov et al., 2018; Cai et al., 2019; Xu et al., 2019). A
69 preliminary description of those multiple sex chromosome systems, including
70 karyotypes, C-bands, rDNA locations, karyotype diversification and identification of
71 sex-specific regions at the cytogenetic level, has been carried out based on
72 conventional cytogenetic (Giemsa-staining and C-banding) and molecular cytogenetic
73 protocols (repetitive DNA markers, comparative genomic hybridization, and whole
74 chromosome painting) (Parise-Maltempi et al., 2007; Cioffi & Bertollo, 2012; Blanco
75 et al., 2013; Sember et al., 2015; Ferreira et al., 2016; Bitencourt et al., 2016).
76 However, adequate genome resources to support more comprehensive descriptions of
77 the multiple sex chromosome system and the origin of the large metacentric Y
78 chromosome of male *O. fasciatus* have been lacking. The recent release of the
79 chromosome-level reference genome of female *O. fasciatus* has provided valuable
80 resource for sex-determination studies, however, a female genome is still need to
81 investigate the origin of the unique X_1X_2Y system for male *O. fasciatus* (Xiao et al.,
82 2019). Using PacBio sequencing and high-throughput chromosome interaction
83 mapping (Hi-C), Xiao et al. (2019) obtained a chromosome-level reference genome of
84 the female *O. fasciatus* with a final size of 768.8 Mb and a contig and scaffold N50
85 length of 2.1 Mb and 33.5 Mb, respectively (Xiao et al., 2019). Twenty-four
86 chromosomes corresponding to the female karyotype ($2n=48$) were assembled at the
87 genome level. Although the high-quality genome of female *O. fasciatus* provides a
88 valuable genomic resource for further study of breeding systems, it could not be used
89 to identify the origin of the large metacentric Y chromosome of male *O. fasciatus*

90 without a male genome.

91 Here, we report the chromosome-level genome assembly of male *O. fasciatus* based
92 on PacBio long-read sequencing and high-throughput chromosome interaction
93 mapping (Hi-C). Genomic comparisons between male and female *O. fasciatus* were
94 carried out to provide insights into the origin of the X₁X₂Y system of male *O.*
95 *fasciatus* based on the chromosome-level genome, which has excellent continuity at
96 the contig and scaffold levels. The genome of male *O. fasciatus* can lay a solid
97 foundation for further study of sex-determining mechanisms of the X₁X₂Y system,
98 and will provide valuable genomic data for conservation genetics and resistance
99 breeding of *Oplegnathus*.

100 **RESULTS**

101 **PacBio sequencing and genome assembly**

102 Two 20 kb PacBio long-read DNA libraries were constructed using the standard
103 protocol provided by the PacBio Sequel platform. A total of ~39.79 Gb of subreads
104 were obtained using SMRT LINK 5.0 to remove the adaptor sequences from the raw
105 data derived from the zero-mode waveguide (**Table 1, Table S1**). Approximately 4.71
106 million sequences with an average length of 8.45 kb were obtained for the draft
107 genome assembly of male *O. fasciatus* (**Table 1**).

108 To increase the continuity and completeness of the genome assembly, four processes
109 were carried out for the contig assembly. First, the Canu v1.4 software was used to
110 assemble an initial genome of male *O. fasciatus* (Koren et al., 2017). As a result, a
111 total length of 866.9 Mb, including 4,453 contigs with a N50 length of 1.73 Mb, was
112 obtained (**Table S2**). Second, Redundans v0.13c software was employed to remove
113 sequence redundancies in the initial assembled genome to obtain a 794.8 Mb genome
114 with a contig N50 length of 2.13 Mb (**Table S2**). Third, Arrow tool implemented in
115 SMRT Link 5.0 software and Pilon v.122 was applied to perform error correction
116 using long read data and Illumina NGS data mentioned in the genome survey analysis
117 (**Table S2**) (Walker et al., 2014; Xiao et al., 2019). The final contig assembly of 795.1
118 Mb with a contig N50 length of 2.13 Mb was obtained. The genome contained 2,295
119 contigs with a longest contig of 9.8 Mb (**Table S2, Table S3**). 881 contigs were longer

120 than 100 kb, representing 92.6% of the total 794.8 Mb for the male *O. fasciatus*
121 genome (**Table 1**). The GC content of the contig assembly genome was 40.87%
122 (**Figure S1, Figure S2**).

123 To obtain the chromosome-level genome of male *O. fasciatus*, the Illumina HiSeq X
124 Ten platform was used to generate ~95.9 Gb clean data from the Hi-C library (**Table**
125 **S1, Table S4**). According to the abovementioned mapping strategy, more than 95.5%
126 of total reads mapped to the assembled genome in pairs, and ~32.5% of read pairs
127 mapped to different contigs. Lachesis software was used to cluster, order and orientate
128 contigs along chromosomes based on their interaction frequencies. As a result, 1,355
129 contigs were successfully anchored and oriented into 23 chromosomes, which was
130 consistent with the previous karyotype analyses of male *O. fasciatus* (X₁X₂Y system)
131 (**Table S4, Figure 1**) (Xu et al., 2012). The total length of anchored contigs was
132 ~762.2 Mb, representing 95.9% of all assembled contigs. Finally, we obtained the
133 chromosome assembly with a contig N50 length of 2.18 Mb and a scaffold N50 length
134 of 32.4 Mb (**Table 1**). Obviously, a large neo-chromosome (*Ch9*) showed strong
135 interaction signals from two genomic blocks, corresponding to the *Ch8* and *Ch10* in
136 female *O. fasciatus* (X₁X₁X₂X₂ system) (**Figure 1**) (Xu et al., 2012). Therefore, *Ch9*
137 was likely to be the large metacentric Y chromosome of male *O. fasciatus*. This
138 chromosome (*Ch9*) was scaffolded from 444 contigs and was 94.2 Mb, more than
139 three times larger than any other chromosomes (**Figure 1, Figure 2, Figure 3**). More
140 than 99.7% of contigs that longer than 100kb were anchored on chromosomes,
141 exhibiting the excellent anchoring rate for male *O. fasciatus* chromosome assembly
142 (**Table S4**).

143 **Genome quality evaluation**

144 The Minimap2 software was employed to evaluate the completeness and homogeneity
145 of the assembled genome of male *O. fasciatus* by using the CLR subreads (**Table S5**).
146 The mapping rate and the coverage of the assembled genome reached 87.6% and
147 99.9%, respectively (**Table S5**). These results showed the high completeness and
148 homogeneity of the genome assembly of male *O. fasciatus*. BUSCO v3.0 software
149 with the actinopterygii_odb9 database was employed to further evaluate the

150 completeness of the assembled genome (Simão et al., 2015). The result showed that
151 97.2% and 1.0% of the 4,456 conserved single-copy orthologous genes were
152 identified as complete BUSCO and fragmented BUSCO profiles in the genome
153 assembly, respectively (**Table 2**). Among the 4,456 conserved single-copy
154 orthologous genes, 4,210 (91.8%) and 246 (5.4%) genes were identified as
155 single-copy and duplicated BUSCOs, respectively (**Table 2**). Approximately 80
156 single-copy orthologous genes were not detected in the actinopterygii_odb9 database.
157 Then, SNP calling data was used to evaluate the accuracy of the male *O. fasciatus*
158 genome assembly, which was generated from the alignment of NGS-based short reads
159 to the assembled genome by using BWA and GATK software. Approximately 1.87
160 million SNP loci were identified, including 1.86 and 0.01 million heterozygous
161 homologous SNPs, respectively (Table S6). The heterozygous SNPs accounted for
162 0.23% of the male *O. fasciatus* genome, which was comparable with our previous
163 study of the heterozygosity for the female *O. fasciatus* genome (Table S6) (Xiao et al.,
164 2019).

165 **Repetitive element identification and protein gene annotation**

166 Approximately 33.5% of the assembled genome was identified as repetitive elements,
167 including repetitive sequences accounting for 23.16% of the male *O. fasciatus*
168 genome based on the *de novo* repeat library (**Table 3**). The estimation of repetitive
169 element content for the male *O. fasciatus* genome were comparable to the result in the
170 *k*-mer analysis (38.4%) (**Table 3**) (Xiao et al., 2019). Interspersed repetitive elements
171 accounting for 22.0% of the male *O. fasciatus* genome were identified, including
172 DNA transposons (10.55%), long interspersed nuclear elements (LINEs, 7.08%) and
173 long terminal repeats (LTRs, 4.11%), respectively (**Table 3, Table S7, Figure S3**).
174 The repetitive contents of the male *Ch9* and the female *Ch8/Ch10* were also identified
175 for 23.79%, 26.07% and 22.70%, respectively (**Table S8**). Although the frequency of
176 DNA transposons, LINEs and LTRs was higher than that in *L. crocea*, *G. aculeatus*,
177 *O. latipes*, and *D. labrax*, the top three categories of TEs were significantly less
178 frequent than in *Epinephelus lanceolatus* and *Triplophysa tibetana* (**Table S7**).
179 Homology-based, *de novo* and transcriptome sequencing-based approaches were

180 integrated to predict protein-coding genes. As a result, 24,835 genes were annotated
181 with an average of 10.0 exons per gene in the male *O. fasciatus* genome (**Table S9**,
182 **Table S10**). The distribution statistics of average gene length, average coding
183 sequence (CDS) length, average exons per gene, average exon length and average
184 intron length of protein-coding genes were also compared to those of six related
185 species (*L. calcarifer*, *L. crocea*, *G. aculeatus*, *G. morhua*, *P. olivaceus* and *C.*
186 *semilaevis*) and showed a similar distribution with those of other teleosts (**Figure S4**,
187 **Table S10**). The average gene length and CDS reached 15,819.4 bp and 1,707.0 bp,
188 respectively (Table S10). Functional annotation of predicted genes in the male *O.*
189 *fasciatus* genome was further performed using the InterPro, Swiss-Prot, TrEMBL, NR,
190 GO and KEGG databases (**Table 4**). Approximately 23,364 of the 24,835 genes
191 (97.34%) in the male *O. fasciatus* genome could be functional annotated by at least
192 one of the abovementioned databases (**Table 4**). We used BUSCO v3.0 software to
193 further evaluate the completeness of the annotated genome against
194 actinopterygii_odb9 in the OrthoDB database (Simão et al., 2015). Approximately
195 96.8% of complete BUSCO genes were successfully identified (**Table 3**). We also
196 used tRNAscan-SE software to annotate the non-coding RNAs against the Rfam
197 database, and 4 types of non-coding RNAs (miRNAs (0.006%), tRNAs (0.009%),
198 rRNAs (0.007%), and snRNAs (0.015%)), including 2666 copies with a total length
199 of 291,392 bp (0.037% of the whole genome) were identified (**Table S11**).

200 **Chromosome comparison of female/male *O. fasciatus***

201 According to the synteny-based chromosome comparison between the male and
202 female *O. fasciatus* genomes using the program MUMmer, we found excellent
203 consistency of genome sequences in corresponding chromosomes (Figure 2, Figure 3).
204 The genome sequences from male *O. fasciatus* had high identity (~99.0%) to those
205 from female *O. fasciatus*, as follows: male *Ch1* / female *Ch1* (99.0%), male *Ch2* /
206 female *Ch2* (99.1%), male *Ch3* / female *Ch3* (99.2%), male *Ch4* / female *Ch4*
207 (99.0%), male *Ch5* / female *Ch5* (99.2%), male *Ch6* / female *Ch6* (99.2%), male *Ch7*
208 / female *Ch7* (99.2%), male *Ch8* / female *Ch9* (99.2%), male *Ch10* / female *Ch11*
209 (99.1%), male *Ch11* / female *Ch12* (99.1%), male *Ch12* / female *Ch13* (99.1%), male

210 *Ch13* / female *Ch14* (99.1%), male *Ch14* / female *Ch15* (99.1%), male *Ch15* / female
211 *Ch16* (99.3%), male *Ch16* / female *Ch17* (99.1%), male *Ch17* / female *Ch18* (99.2%),
212 male *Ch18* / female *Ch19* (99.2%), male *Ch19* / female *Ch20* (99.1%), male *Ch20* /
213 female *Ch21* (99.1%), male *Ch21* / female *Ch22* (99.2%), male *Ch22* / female *Ch23*
214 (99.2%), male *Ch23* / female *Ch24* (99.2%). The comparisons of chromosomal
215 sequences of female *Ch8/Ch10* and the male *Ch9* were further performed (Figure 3 b).
216 A total of ~31.3 Mb homology sequences for female *Ch8* were aligned to male *Ch9*
217 with a high identity (~99.0%), representing 83.4% of the whole *Ch8* length (37.5 Mb)
218 (**Table S12**). Similarly, more than 90.1% of *Ch10* sequences exhibited a high identity
219 with male *Ch9* (Table S12). Meanwhile, approximately 67.0% sequences (63.1 Mb)
220 of the male *Ch9* (94.2 Mb) showed a high identity (~99.0%) with those from the
221 female *Ch8* and *Ch10* using nucmer with minimum match length of 1000 bp (**Table**
222 **S12**). After reducing the parameter of minimum match length to 100 bp, we observed
223 that more than 89.5% of the male *Ch9* could align to the female *Ch8* and *Ch10*,
224 suggesting that the male *Ch9* might undergo massive rearrangements during the
225 neo-Y chromosome formation (**Table S13, Figure S5**). Indeed, structure variations
226 (SV) were identified in sequences for the male *Ch9* lacking homolog to the female
227 *Ch8* and *Ch10*, including 72 breakpoints, 7 translocations, 26 relocations and 23
228 inversions (**Figure 2c**).

229 According to homology searching of genes in the male genome to the female genome,
230 we identified 172 male-specific genes in the male *Ch9*. Several genes involved in the
231 chromosome organization and nucleosome assembly processes for fish, such as
232 chromosome transmission fidelity protein 8 (*ctf8*), centromere protein P (*cenpp*),
233 synaptonemal complex protein 1 (*sycp1*), caveolin 3 (*cav3*) (**Table S14**). The *ctf8*
234 could regulate sister chromatid cohesion and fidelity of chromosome transmission
235 (Bermudez et al., 2003). The *cenpp* involves in assembly of kinetochore proteins,
236 mitotic progression and chromosome segregation (Okada et al., 2006). The *sycp1* is as
237 major component of the transverse filaments of synaptonemal complexes and formed
238 between homologous chromosomes during meiotic prophase (Bisig et al., 2012). The
239 functions of *cav3* could serve as a component of the caveolae plasma membranes in

240 most cell types (Shang et al., 2019).

241 The conservation synteny analysis for male - female *O. fasciatus* comparison and *O.*
242 *fasciatus* (the X_1X_2Y system) - *O. latipes* (the normal XY system) comparison using
243 homolog gene-pairs between two species were also performed. As a result,
244 twenty-two of female *O. fasciatus* chromosomes harbored an excellent one-to-one
245 correspondence to those of the male *O. fasciatus* genome excepted for female *Ch8*
246 and *Ch10*. The male *Ch9* showed strong conserved synteny with female *Ch8* and
247 *Ch10*, consistent with the abovementioned results that *Ch9* might be the neo-Y
248 chromosome (**Table S15, Figure 3, Figure 4, Figure S6**). Furthermore, we found
249 that the synteny of chromosomes for *O. fasciatus* and *O. latipes* were largely
250 conserved. Fourteen chromosomes of male *O. fasciatus* genome were unambiguously
251 aligned to single chromosomes of *O. latipes* genome (**Table S15, Figure 4**). Other 9
252 chromosomes of the male *O. fasciatus* genome exhibited several small
253 inter-chromosome conservation synteny to *O. latipes* chromosomes, suggesting that
254 massive inter-chromosome rearrangements occurred after divergence of two species
255 (**Table S15, Figure 4**). We found that *Ch5* and *Ch6* in the *O. latipes* genome
256 exhibited excellent synteny with female *Ch8* and *Ch10*, as well as with *Ch9* of male *O.*
257 *fasciatus* (**Table S15, Figure 4, Figure S6**).

258 The syntenic blocks of the chromosomes were also evaluated among the male/female
259 *O. fasciatus* and *L. crocea* genomes using the program MUMmer. The consistency of
260 chromosomes, with 24 blocks between female *O. fasciatus* and *L. crocea* and 23
261 blocks among male *O. fasciatus*, *L. crocea* and female *O. fasciatus*, was detected
262 (**Figure 3**). Precise pairings of protein-coding genes originating from the male and
263 female *O. fasciatus* chromosomes were established using BLASTP software with
264 identity $\geq 95\%$ (coverage $\geq 90\%$) and e-value $\leq 1E-5$. The results showed that 10,919
265 protein-coding genes pairs were identified, 1,459 of which were located on the large
266 neo-chromosome (*Ch9*) in the male genome, corresponding to 809 genes of *Ch8* and
267 628 genes of *Ch10* in the female genome, respectively (**Figure 3**).

268 **Gene family identification and phylogenetic tree construction**

269 According to the homolog searching of protein-coding genes for male *O. fasciatus*

270 and other species, including *S. salar*, *L. crocea*, *G. morhua*, *P. olivaceu*, *C. semilaevis*,
271 *N. coriiceps*, *B. pectinirostris*, *B. floridae*, *G. aculeatus*, *C. milii*, *D. rerio* and *O.*
272 *latipes*, approximately 23,302 gene families were identified based on their H-scores
273 (**Figure S7**). The specific and common gene families of male *O. fasciatus* and other
274 teleosts (*L. crocea*, *G. morhua* and *S. salar*) were further analyzed, which yielded 551
275 specific gene families in the male genome and 11,484 common gene families among
276 the four teleosts (**Figure S8**). Using the MCL program implemented in the OrthoMCL
277 pipeline with a coefficient setting of 1.5 to cluster the abovementioned gene families,
278 we obtained 810 single-copy genes, which were employed to reconstruct the
279 phylogenetic relationships among male *O. fasciatus* and the other species. Based on a
280 length filter that retained protein sequences ≥ 100 aa, 759 single-copy orthogroups
281 were obtained using ClustalW software to extract and align single-copy genes from
282 the 810 single-copy orthogroups (**Figure S7**). The multiple sequence alignment for
283 the filtered single-copy genes was performed using MUSCLE software, and a
284 super-alignment data set for each species was obtained and used to construct a
285 phylogenetic tree of the male *O. fasciatus* and the other species based on the
286 maximum-likelihood method implemented in the RAxML package (**Figure 5**). The
287 results of the phylogenetic tree showed that *O. fasciatus* from the Oplegnathidae
288 family of the Centrarchiformes (Eupercaria) was close to *Larimichthys crocea* in the
289 order Perciformes (Eupercaria), consistent with the new phylogenetic classification of
290 bony fishes (**Figure 5**) (Betancur-R et al., 2017). The divergence times among clades
291 were evaluated using the MCMCtree program with calibration times based on the
292 TimeTree database, showing that *O. fasciatus* diverged from its common ancestor
293 with *Larimichthys crocea* approximately 62.8-73.4 million years ago (Figure 5).

294 DISCUSSION

295 *O. fasciatus* is an important fishery species in offshore cage aquaculture and fish
296 stocking for marine ranching in East Asia (Schembri et al., 2010; Xiao et al., 2016;
297 Xiao et al. 2019). The male *O. fasciatus* genome was characterized by an X₁X₂Y
298 system with a neo-Y chromosome based on male karyotype analyses. The species
299 could be used as an excellent model to address the sex determination, origin and

300 evolution of the X_1X_2Y system. The chromosome-level genome of male *O. fasciatus*
301 assembled in the present study, combined with the released reference genome of
302 female *O. fasciatus*, will provide valuable genomic resources to gain insights into the
303 origin of the X_1X_2Y system (Xiao et al., 2019).

304 To assess the quality of the assembly, the continuity and completeness of the genome
305 was evaluated. The final contig assembly was 795.1 Mb with a contig N50 length of
306 2.13 Mb for male *O. fasciatus*, which was comparable to those of the female (Xiao et
307 al., 2019). The contig N50 values of the male/female *O. fasciatus* genomes were also
308 larger than those of many reported teleost genomes, which indicated that high genome
309 continuity existed in *O. fasciatus* genomes (**Table S3**). 1,355 ordered contigs were
310 scaffolded into 23 chromosomes, yielding a final chromosome-level genome of
311 approximately 762 Mb with a scaffold N50 length of 32.43 Mb (**Table 1**). The
312 completeness of the assembled genome was evaluated using BUSCO. The high
313 continuity and completeness of the male *O. fasciatus* genome will lay a solid
314 foundation for further studies of population genetics, evolutionary of genome
315 comparisons, neo-chromosome structure and sex-determining mechanisms (Sun et al.,
316 2017; Yang et al., 2018; Sun et al., 2019).

317 So far, 37 species have been reported to possess multiple sex chromosomes with
318 $X_1X_1X_2X_2/X_1X_2Y$ system among teleosts. Although techniques, such as Giemsa
319 staining, C-banding, repetitive DNA markers, CGH and WCP, have been used for the
320 chromosomal studies, the origination of the neo-Y chromosome of *O. fasciatus* in
321 previous studies were still largely hindered by the lack of reference genome resources,
322 especially for the neo-Y chromosome (Sember et al., 2015; Bitencourt et al., 2016;
323 Zhang et al., 2018; Krysanov et al., 2018; Cai et al., 2019; Xu et al., 2019). In this
324 work, a large neo-chromosome (*Ch9*) was assembled into 94.2 Mb, corresponding to
325 the large metacentric Y chromosome of male *O. fasciatus*. The neo-chromosome
326 could be responsible for the genome size discrepancy between male and female *O.*
327 *fasciatus* (**Table S4, Figure 1**).

328 Three proposed mechanisms for the origin of an X_1X_2Y multiple sex chromosome
329 system have been postulated, which included fusion between the Y chromosome and

330 an autosome, fission of the X chromosome, and reciprocal translocation between the
331 X chromosome and an autosome, respectively (White et al., 1983; Kitano & Peichel,
332 2012). All those mechanisms (fusion and fission) could induce remarkable genome
333 size changes for sex chromosomes (Y, X), leading to a large neo-Y chromosome or a
334 small neo-X chromosome (Kitano & Peichel, 2012). Previous studies have shown that
335 the X_1X_2Y systems of teleosts mainly originate from chromosomal fusions, leading to
336 large metacentric chromosomes (neo-Y chromosomes) through a Robertsonian fusion
337 of two acrocentric chromosomes (the Y chromosome and an autosome) (Uyeno &
338 Miller, 1971; Bertollo et al. 2000; Bertollo et al., 2004; Ueno & Takai, 2008; Kitano
339 & Peichel, 2012). Although the formation of the X_1X_2Y multiple sex chromosome
340 system could be achieved through fission of the X chromosome, this process would
341 lead to an increase in the diploid number of chromosomes (e. g., female $2n=50$, male
342 $2n=49$) compared with the ancestral karyotype of marine teleost ($2n=48$) (White et al.,
343 1983; Kitano & Peichel, 2012). Our genome assembly for males and females of *O.*
344 *fasciatus* lead to 23 and 24 chromosomes, directly corresponding to the male and
345 female karyotypes ($2n=47/48$), respectively (**Figure 1, Figure 2**) (Xu et al., 2012;
346 Xiao et al., 2019). The comparative analysis showed excellent chromosomal synteny
347 between the male and female *O. fasciatus* genomes (**Figure 1, Figure 2, Figure 3**).
348 No small neo-X chromosome was observed at the genome level; however, a large
349 neo-Y chromosome (*Ch9*) (63.1 Mb/94.2 Mb) in the male *O. fasciatus* genome
350 exhibited high identity (~99.0%) to those of the female chromosomes *Ch8* and *Ch10*.
351 From the chromosomal comparison, *O. fasciatus* female *Ch8* and *Ch10* exhibited
352 excellent synteny with those of *Ch5* and *Ch6* in *O. latipes* genome, indicating *Ch8*
353 and *Ch10* in *O. fasciatus* likely separated in their common ancestor (**Table S12**).
354 According to the sequence and synteny comparison and previous karyotypes results,
355 we suggested that a centric fusion of acrocentric chromosomes *Ch8* and *Ch10* should
356 be responsible for the formation of the X_1X_2Y system of male *O. fasciatus*.
357 Neo-sex chromosome systems are always derived from rearrangements between
358 original sex chromosomes and autosomes through chromosomal fissions,
359 fragmentations and fusions (Uyeno & Miller, 1971; Bertollo et al., 2000; Bertollo et

360 al., 2004; Ueno & Takai, 2008; Kitano & Peichel; 2012). Indeed, although the male
361 large neo-chromosome *Ch9* showed general excellent synteny with the female
362 *Ch8/Ch10*, several obvious rearrangements were also observed at the middle of the
363 chromosomes between *Ch9* and *Ch8/Ch10*, especially for flanking regions of
364 breakpoints around 18 Mb~20 Mb, 28 Mb~32 Mb and 39 Mb~47 Mb in male *Ch9*
365 (**Figure 2**). Cross-chromosome synteny were also identified between the male *Ch9* of
366 *O. fasciatus* and the *Ch5/Ch6* of *O. latipes* genome, which exhibited excellent synteny
367 with female *Ch8* and *Ch10* of *O. fasciatus* (**Figure 4**). These results showed that
368 chromosome rearrangements events have occurred in the neo-chromosome *Ch9* of
369 male *O. fasciatus*.

370 The neo-chromosomes of the X_1X_2Y system could also participate in sex regulation
371 and determination (Ueno & Takai 2008; Shao et al., 2012). Previous studies showed
372 that neo-chromosomes might harbor important genes or regulatory elements
373 responsible to the behaviors, phenotype and speciation (Kitano et al., 2009). Some
374 male-specific genes involved in chromosome and nucleosome assembly (*ctf8*, *cenpp*,
375 *sycp1*) and steroid hormone synthesis (*nr4a1*) were identified in the present study,
376 which might be responsible for the fidelity of homologous chromosome pairing
377 between *Ch9* and *Ch8/Ch10* during meiotic prophase and male sex determination
378 (**Table S14**). This high-quality chromosome-level genome will enable us to explore
379 the fusion mechanism and biological functions of neo-chromosomes by analyses for
380 the genetic composition and chromosome conformation studies based on the Hi-C.
381 The multiple sex chromosome system with sexual dimorphism could also lead to
382 growth differences. Sexual dimorphism on the growth has been detected in *O.*
383 *fasciatus* that male fish grow faster than females (Chen et al., 2014; Xiao et al. 2015).
384 A total of 24,105 protein-coding genes were functionally annotated for the
385 chromosome-level genome of male *O. fasciatus*, and these genes will serve as a
386 framework combined with quantitative trait locus (QTL) and bulked segregant
387 analysis (BSA) techniques for studies of growth regulation and breeding.

388 In summary, we have successfully completed a chromosome-level genome assembly
389 for male *O. fasciatus* and first assembled the large neo-chromosome corresponding to

390 the karyotype of male *O. fasciatus* with high continuity and completeness. This study
391 demonstrated for the first time that the X₁X₂Y system of male *O. fasciatus* originated
392 from the fusions of the non-homologous chromosomes *Ch8* and *Ch10* via significant
393 homology and chromosomal interactions at the genome level. This high-quality
394 genome assembly will not only provide a solid foundation for further sex-determining
395 mechanism research in the X₁X₂Y system, but also facilitate the artificial breeding
396 aiming to improve the yield and disease resistance for *Oplegnathus*.

397

398 **Limitations of study**

399 The chromosomes fusion was suggested to be responsible for the formation of the
400 X₁X₂Y system only from the male *O. fasciatus*, the extremely limited genome
401 information of the fishes with multiple sex chromosomes led to difficulties in
402 accurately determining the dynamics and mechanism of chromosome fusions.

403 **METHODS**

404 All methods can be found in the accompanying Transparent Methods supplemental
405 file.

406 **DATA AND CODE AVAILABILITY**

407 The RNA sequencing data of the *Oplegnathus fasciatus* has been deposited in the
408 SRA under Bioproject number PRJNA486572. The whole genome sequencing data
409 are available in the NCBI with the accession number SRP220007.

410 **SUPPLEMENTAL INFORMATION**

411 Supplemental Information can be found online at
412 <http://dx.doi.org/10.17632/5xtt3d9btm.3>

413 **ACKNOWLEDGEMENTS**

414 This study was supported by a grant from the National Natural Science Foundation of
415 China (No. 41506170, No. 31672672, and No. 31872195), National Key Research and
416 Development Program (2018YFD0901204), STS project (KFZD-SW-106, ZSSD-019,
417 2017T3017, KFJ-STQ-QYZX-020), Qingdao National Laboratory for Marine Science
418 and Technology (2018SDKJ0502-2, 2015ASKJ02), China Agriculture Research
419 System (CARS-47), Shandong Province Key Research and Invention Program

420 (2017GHY15102, 2017GHY15106), Qingdao Source Innovation Program
421 (17-1-1-57-jch), Marine Fishery Institute of Zhejiang Province, Key Laboratory of
422 Mariculture and Enhancement of Zhejiang Province (2016KF002).

423 AUTHOR CONTRIBUTIONS

424 Y.S.X. conceived the project. Z.Z.X., D.Y.M., J.L. collected the samples and extracted
425 the genomic DNA. Y.S.X., J.L., C.X.Z., H.W., L.L., W.C.N., S.J.X. and J.L.
426 performed the genome assembly and data analysis. Y.S.X., Z.Z.X., S.J.X., J.L., D.Y.M.
427 and J.L. wrote the paper. A.H. polished the paper.

428 DECLARATION OF INTERESTS

429 The authors declare no competing interests.

430

431 FIGURE LEGENDS

432 **Figure 1. Genome assembly of female and male *O. fasciatus* based on the Hi-C**
433 **interaction analyses. (a)** The heatmap of interactions among genomic bins of 500 kb
434 along 24 chromosomes for female *O. fasciatus* (The data was cited from the reference
435 (Xiao et al. 2019). **(b)** The heatmap of interactions among genomic bins of 500 kb along
436 23 chromosomes for male *O. fasciatus*. **(c)** The cumulative distribution of subtraction
437 Hi-C Z-scores for interactions between 400 kb and 40 kb bins from the whole genome
438 and chromosome levels. Blocks represent the interactions among genomic bins and
439 the interaction strength was represented by the color scheme from deep (strong
440 interactions) to light (weak interactions). A large neo-chromosome (*Ch9*) was
441 assembled in the male *O. fasciatus* reference genome.

442 **Figure 2. Genomic comparisons between female and male *O. fasciatus*. (a)**
443 Genomic comparisons of the whole genome by direct sequence alignment. The
444 majority of female and male *O. fasciatus* chromosomes exhibited 1:1 correspondence
445 except for the large neo-chromosome (*Ch9*). **(b)** Detailed genomic comparisons
446 between *Ch9* and *Ch8/Ch10* from male and female genomes. The large
447 neo-chromosome (*Ch9*) of the male *O. fasciatus* genome showed largely synteny with
448 the *Ch8* and *Ch10* of the female *O. fasciatus* genome. **(c)** The statistics of structure
449 variants (SV) with length more than 10 kb between *Ch9* and *Ch8/Ch10* from male and

450 female genomes.

451 **Figure 3. Genome comparisons among male/female *O. fasciatus* and *L. crocea*. (a)**

452 From outer to inner circles: A, 23 chromosomes of male *O. fasciatus*; B, 24

453 chromosomes of *L. crocea*. The yellow color represents the whole chromosomes and

454 the red lines in the yellow areas represent the common chromosomal region with the

455 male *O. fasciatus*. C, 24 chromosomes of female *O. fasciatus*. The yellow color

456 represents the whole chromosome and the blue lines in the yellow areas represent the

457 common chromosomal region with the male *O. fasciatus*. D, 23 chromosomes of male

458 *O. fasciatus*. The red color represents the whole chromosome and the yellow lines in

459 the red areas represent the common chromosomal region with the female *O. fasciatus*

460 and *L. crocea*. E, the red color represents the chromosomes of female *O. fasciatus* and

461 the green color represents the male *O. fasciatus*. Each lines precisely joined pair of

462 genes originated from the male and female *O. fasciatus* chromosomes. (b) and (c)

463 From outer to inner circles: a, the 9th chromosome (*Ch9*) of male *O. fasciatus* with

464 coordinate. b, the distribution of forward protein-coding genes in male *Ch9*. c, the

465 distribution of reverse protein-coding genes in male *Ch9*. d, the chromosomal region

466 of male *Ch9* aligned to *Ch8* of female *O. fasciatus* with red color. e, the chromosomal

467 region of male *Ch9* aligned to *Ch10* of female *O. fasciatus* with green color. The gray

468 color represents the distribution of protein-coding genes in unique genomic regions of

469 male *Ch9* (b, c tracks of figure (b)). The color gradient corresponds to the degree of

470 similarities for male *Ch9* genes with the female genes in the b, c track of figure (c).

471 **Figure 4. Chromosome conserved synteny between *Oryzias latipes* genome (the**

472 **normal XY system) and *O. fasciatus* genome (the X₁X₂Y system).** Ribbons

473 between two genomes represented chromosomal conservation synteny blocks.

474 **Figure 5. Phylogenetic analysis of male *O. fasciatus* and other related 12 species.**

475 21,528 gene families were identified by clustering the homologous gene sequences,

476 and 810 single-copy orthogroups were obtained, 719 filtered single-copy orthogroups

477 were used to construct the phylogenetic relationship between *O. fasciatus* and other

478 species (*S. salar*, *L. crocea*, *G. morhua*, *P. olivaceus*, *C. semilaevis*, *N. coriiceps*,

479 *B. pectinirostris*, *B. floridae*, *G. aculeatus*, *C.milii*, *D. rerio* and *O. latipes*).
480 Divergence times among the species (red dots) from TimeTree database were used as
481 the calibration divergence times. Blue values on branches indicated the estimated
482 divergence time in millions of years ago (Mya), and numbers in parentheses showed
483 the interval of 95% confidence.

484

485 REFERENCE

486 Altschul, S.F., Gish, W., Miller, W., Myers, E.W., and Liponan, D.J. (2012). Basic local alignment
487 search tool (BLAST). *J. Mol. Biol.* 215, 403-410.

488 Belaghzal, H., Dekker, J., and Gibcus, J.H. (2017). HI-C 2.0: An optimized Hi-C procedure for
489 high-resolution genome-wide mapping of chromosome conformation. *Methods* 123, 56-65.

490 Benson, G. (1999). Tandem repeats finder: A program to analyze DNA sequences. *Nucleic Acids*
491 *Res.* 27, 573.

492 Bertollo, L.A.C., Born, G.G., Dergam, J.A., Fenocchio, A.S., and Moreira-Filho, O. (2000). A
493 biodiversity approach in the neotropical Erythrinidae fish, *Hoplias malabaricus*. Karyotypic
494 survey, geographic distribution of cytotypes and cytotaxonomic considerations. *Chromosome Res.*
495 8, 603-613.

496 Bertollo, L.A.C., Oliveira, C., Molina, W.F., Margarido, V.P., Fontes M.S., Pastori, M.C., and
497 Fenocchio, A.S. (2004). Chromosome evolution in the erythrinid fish, *Erythrinus erythrinus*
498 (Teleostei: Characiformes). *Heredity* 93, 228-233.

499 Betancur-R, R., Wiley, E.O., Arratia, G., Acero, A., Bailly, N., Miya, M., Lecointre, G., and Ortí,
500 G. (2017). Phylogenetic classification of bony fishes. *BMC Evol. Biol.* 17, 162.

501 Birney, E., Clamp, M., and Durbin, R.J. (2004). GeneWise and genomewise. *Genome Res.* 14,
502 988.

503 Bitencourt, J.A., Sampaio, I., Ramos, R.T.C., Vicari, M.R., and Affonso, P.R.A.M. (2016). First
504 report of sex chromosomes in Achiridae (Teleostei: Pleuronectiformes) with inferences about the
505 origin of the multiple $X_1X_1X_2X_2/X_1X_2Y$ system and dispersal of ribosomal genes in *Achirus*
506 *achirus*. *Zebrafish* 14, 90-95.

507 Blanco, D.R., Vicari, M.R., Lui, R.L., Bertollo, L.A.C., Traldi, J.B., and Moreira-Filho, O. (2013).
508 The role of the Robertsonian rearrangements in the origin of the XX/XY_1Y_2 sex chromosome

- 509 system and in the chromosomal differentiation in *Harttia* species (Siluriformes, Loricariidae). Rev
510 Fish Biol Fisher 23, 127-134.
- 511 Burge, C., and Karlin, S. (1997). Prediction of complete gene structures in human genomic DNA.
512 J. Mol. Biol. 268, 78-94.
- 513 Burton, J.N., Adey, A., Patwardhan, R.P., Qiu, R., Kitzman, J.O., and Shendure, J. (2013).
514 Chromosome-scale scaffolding of de novo genome assemblies based on chromatin interactions.
515 Nat. Biotechnol. 31, 1119-1125.
- 516 Bermudez, V.P., Maniwa, Y., Tappin, I., Ozato, K., Yokomori, K., Hurwitz, J. (2003). The
517 alternative Ctf18-Dcc1-Ctf8-replication factor C complex required for sister chromatid cohesion
518 loads proliferating cell nuclear antigen onto DNA. Proc. Natl. Acad. Sci. USA 100, 10237-10242.
- 519 Bisig, C.G., Guiraldelli, M, F., Kouznetsova, A., Scherthan, H., Höög, C., Dawson, D.S., and
520 Pezza, R. J. (2012). Synaptonemal complex components persist at centromeres and are required
521 for homologous centromere pairing in mouse spermatocytes. Plos Genet. 8, e1002701.
- 522 Cai, M.Y., Xiao, S.J., Li, W.B., Han, Z.F., Han, F., Xiao, J.Z., Liu, F.L., and Wang, Z.Y. (2019).
523 Chromosome assembly of *Collichthys lucidus*, a fish of Sciaenidae with a multiple sex
524 chromosome system. Sci. Data 6, 132.
- 525 Campbell, M.S., Holt, C., Moore, B., and Yandell, M. (2014). Genome Annotation and Curation
526 Using MAKER and MAKER-P. Curr. Protoc. Bioinformatics 48, 4.11.11.
- 527 Chen, S.L., Zhang, G.J., Shao, C.W., Huang, Q.F., Liu, G., Zhang, P., Song, W.T., An, N.,
528 Chalopin, D., Volf, J.N., et al. (2014). Whole-genome sequence of a flatfish provides insights into
529 ZW sex chromosome evolution and adaptation to a benthic lifestyle. Nature 46, 253-260.
- 530 Chin, C.S., Alexander, D.H., Marks, P., Klammer, A.A., Drake, J., Heiner, C., Clum, A., Copeland,
531 A., Huddleston, J., Eichler, E.E., Turner, S.W., and Korlach, J. (2013). Nonhybrid, finished
532 microbial genome assemblies from long-read SMRT sequencing data. Nat. Methods 10, 563.
- 533 Cioffi, M.B., and Bertollo, L.A.C. (2012). Chromosomal distribution and evolution of repetitive
534 DNAs in fish. Repetit. DNA 7, 197-221.
- 535 Conesa, A., Götz, S., García-Gómez, J.M., Terol, J., Talón, M., and Robles, M. (2005). Blast2GO:
536 universal tool for annotation, visualization and analysis in functional genomics research.
537 Bioinformatics 21, 3674.
- 538 Delcher, A.L., Salzberg, S.L., and Phillippy, A.M. (2003). Using MUMmer to identify similar

539 regions in large sequence set. *Current Protocol in Bioinformatics Chapter 10: Unit 10.3.*

540 Durand, N.C., Shamim, M.S., Machol, I., Rao S.S.P., Huntley, M.H., Lander, E.S., and Aiden E.L.
541 (2016). Juicer provides a one-click system for analyzing loop-resolution Hi-C experiments. *Cell*
542 *Syst.* 3, 95-98.

543 Edgar, R.C. (2004). MUSCLE: multiple sequence alignment with high accuracy and high
544 throughput. *Nucleic Acids Res.* 32, 1792-1797.

545 Ferreira, M., Garcia, C., Matoso, D.A., de Jesus, I.S., and Feldberg, E. (2016). A new multiple sex
546 chromosome system X1X1X2X2/X1Y1X2Y2 in Siluriformes: Cytogenetic characterization of
547 *Bunocephalus coracoideus* (Aspredinidae). *Genetica* 144, 591-599.

548 Flicek, P., Amode, M.R., Barrell, D., Beal, K., Billis, K., Brent, S., Carvalho-Silva, D., Clapham,
549 P., Coates, G., Fitzgerald, S., et al. (2014). Ensembl 2014. *Nucleic Acids Res.* 42 (Database
550 issue), D749–D755.

551 Griffiths-Jones, S., Bateman, A., Marshall, M., Khanna, A., and Eddy, S.R. (2003). Rfam: An RNA
552 family database. *Nucleic Acids Res.* 31, 439-441.

553 Harris, M.A., Clark, J., Ireland, A., Lomax, J., Ashburner, M., Foulger, R., Eilbeck, K., Lewis, S.,
554 Marshall, B., Mungall, C., et al. (2004). The Gene Ontology (GO) database and informatics
555 resource. *Nucleic Acids Res.* 32, 258D-261.

556 Jaillon, O., Aury, J.M., Brunet, F., Petit, J.L., Stange-Thomann, N., Mauceli, E., Bouneau, L.,
557 Fischer, C., Ozouf-Costaz, C., Bernot, A., et al. (2004). Genome duplication in the teleost fish
558 *Tetraodon nigroviridis* reveals the early vertebrate protokaryotype. *Nature* 431, 946.

559 Kasahara, M., Naruse, K., Sasaki, S., Nakatani, Y., Wei, Q., Ahsan, B., Yamada, T, Nagayasu, Y,
560 Doi, K., Kasai, Y., et al. (2007). The medaka draft genome and insights into vertebrate genome
561 evolution. *Nature* 447, 714-719.

562 Kitano, J., and Peichel, C. (2012). Turnover of sex chromosomes and speciation in fishes. *Environ.*
563 *Biol. Fish.* 94, 549-558.

564 Koren, S., Walenz, B.P., Berlin, K., Miller, J.R. Bergman, N.H., and Phillippy, A.M. (2017). Canu:
565 scalable and accurate long-read assembly via adaptive *k*-mer weighting and repeat separation.
566 *Geneome Res.* 27, 722-736.

567 Krysanov, E. and Demidova, T. (2018). Extensive karyotype variability of African fish genus
568 *Nothobranchius* (Cyprinodontiformes). *Comp. Cytogenet.* 12, 387-402.

- 569 Krzywinski, M., Schein, J., Birol, I., Connors, J., Gascoyne, R., Horsman, D., Jones, S.J., and
570 Marra, M.A. (2009). Circos: An information aesthetic for comparative genomics. *Genome Res.*
571 *19*, 1639-1645.
- 572 Kurtz, S., Phillippy, A., Delcher, A., Smoot, M., Shumway, M., Antonescu, C., and Salzberg, S.L.
573 (2004). Versatile and open software for comparing large genomes. *Genome Biol.* *5*, R12.
- 574 Li, H. (2018). Minimap2: pairwise alignment for nucleotide sequences. *Bioinformatics* *34*,
575 3094-3100.
- 576 Li, H., and Durbin, R. (2009). Fast and accurate short read alignment with Burrows–Wheeler
577 transform. *Bioinformatics* *25*, 1754-1760.
- 578 Li, H., Sun, Z.P., Li, Q., and Jiang, Y.L. (2011). Characterization of an Iridovirus Detected in Rock
579 Bream (*Oplegnathus fasciatus*; Temminck and Schlegel). *Chin. J. Virol.* *27*, 158-164.
- 580 Li, L., Stoeckert, C.J., and Roos, D.S. (2003). OrthoMCL: Identification of Ortholog Groups for
581 Eukaryotic Genomes. *Genome Res.* *13*, 2178-2189.
- 582 Lobo, I. (2008). Basic local alignment search tool (BLAST). *Nature Educat.* *1*.
- 583 Lowe, T.M., and Eddy, S.R. (1997). tRNAscan - SE: A program for improved detection of transfer
584 RNA genes in genomic sequence. *Nucleic Acids Res.* *25*, 955-964.
- 585 Marçais, G., and Kingsford, C. (2011). A fast, lock-free approach for efficient parallel counting of
586 occurrences of k-mers. *Bioinformatics* *27*, 764.
- 587 McKenna, A., Hanna, M., Banks, E., Sivachenko, A., Cibulskis, K., Kernysky, A., Garimell, K.,
588 Altshuler, D., Gabriel, S., Daly, M., et al. (2010). The Genome Analysis Toolkit: A MapReduce
589 framework for analyzing next-generation DNA sequencing data. *Genome Res.* *20*, 1297-1303.
- 590 Ogata, H., Goto, S., Sato, K., Fujibuchi, W., Bono, H., and Kanehisa, M. (2000). KEGG: kyoto
591 encyclopedia of genes and genomes. *Nucleic Acids Res.* *27*, 29-34.
- 592 Okada, M., Cheeseman, I.M., Hori, T., Okawa, K., McLeod, I.X., Yates, J. R., Desai, A., and
593 Fukagawa, T. (2006). The CENP-H-I complex is required for the efficient incorporation of newly
594 synthesized CENP-A into centromeres. *Nat Cell Biol.* *8*, 446-457.
- 595 Parise-Maltempo, P.P., Martins, C., Oliveira, C., and Foresti, F. (2007). Identification of a new
596 repetitive element in the sex chromosomes of *Leporinus elongatus* (Teleostei: Characiformes:
597 Anostomidae): new insights into the sex chromosomes of *Leporinus*. *Cytogenet Genome Res.* *116*,

598 218-223.

599 Park, H.S., Kim, C.G., Kim, S., Park, Y.J., Choi, H.J. Xiao, Z.Z., Li, J., Xiao, Y.S., and Lee, Y.H.
600 (2018). Population Genetic Structure of Rock Bream (*Oplegnathus fasciatus* Temminck &
601 Schlegel, 1844) Revealed by mtDNA COI Sequence in Korea and China. *Ocean. Sci. J.* 53,
602 261-274.

603 Prysycz, L.P., and Gabaldón, T. (2016). Redundans: an assembly pipeline for highly heterozygous
604 genomes. *Nucleic Acids Res.* 44, e113-e113.

605 Schembri, P.J., Bodilis, P., Evans, J., and Francour, P. (2010). Occurrence of barred
606 kinfejaw, *Oplegnathus fasciatus* (Actinopterygii: Perciformes: Oplegnathidae), in Malta (Central
607 Mediterranean) with a discussion on possible modes of entry. *Acta Ichthyol. Piscat.* 40, 101-104.

608 Sember, A., Bohlen, J., Šlechtová, V., Altmanová, M., Symonová, R. and Ráb, P. (2015).
609 Karyotype differentiation in 19 species of river loach fishes (Nemacheilidae, Teleostei): Extensive
610 variability associated with rDNA and heterochromatin distribution and its phylogenetic and
611 ecological interpretation. *BMC Evol. Biol.* 15, 251-272.

612 Simão, F.A., Waterhouse, R.M., Ioannidis, P., Kriventseva, E.V., and Zdobnov E.M. (2015).
613 BUSCO: assessing genome assembly and annotation completeness with single-copy orthologs.
614 *Bioinformatics* 31, 3210-3212.

615 Stamatakis, A. (2014). RAxML version 8: a tool for phylogenetic analysis and post-analysis of
616 large phylogenies. *Bioinformatics* 30, 1312-1313.

617 Stanke, M., Steinkamp, R., Waack, S., and Morgenstern, B. (2004). AUGUSTUS: a web server for
618 gene finding in eukaryotes. *Nucleic Acids Res.* 32, W309-W312.

619 Sanyal, A., Lajoie, B.R., Jain, G. and Dekker, J. (2012). The long-range interaction landscape of
620 gene promoters. *Nature* 489, 109-113.

621 Shang, L., Chen, T., Xian, J., Deng, Y., Huang, Y., Zhao, Q., Liang, G., Liang, Z., Lian, F., Wei, H.,
622 and Huang, Q. (2019). The caveolin-3 P104L mutation in LGMD-1C patients inhibits
623 non-insulin-stimulated glucose metabolism and growth but promotes myocyte proliferation. *Cell*
624 *Biol. Int.* 43, 669-677.

625 Sun, J., Zhang, Y., Xu, T., Zhang, Y., Mu, H., Zhang, Y., Lan, Y., Fields, C.J., Hui, J.H.L., Zhang,
626 W., et al., (2017). Adaptation to deep-sea chemosynthetic environments as revealed by mussel
627 genomes. *Nat. Ecol. Evol.* 1, 121.

- 628 Sun, J., Mu, H.W., CH Ip, J., Li, R.S., Xu, T., Accorsi, A., Sánchez Alvarado, A., Ross, E., Lan, Y.,
629 Sun, Y.N., et al. (2019). Signatures of Divergence, Invasiveness, and Terrestrialization Revealed
630 by Four Apple Snail Genomes. *Mol. Biol. Evol.* 36, 1507-1520.
- 631 Tarailo-Graovac, M., and Chen, N. (2009). Using RepeatMasker to identify repetitive elements in
632 genomic sequences. *Current Protocols in Bioinformatics*, Chapter 4, Unit 4.10.
- 633 Thompson, J.D., Gibson, T.J., and Higgins, D.G. (2002). Multiple sequence alignment using
634 ClustalW and ClustalX. *Current Protocols in Bioinformatics*, 4.10.1-4.10.14 1-14.
- 635 Trapnell, C, Pachter, L., and Salzberg, S.L. (2009). TopHat: discovering splice junctions with
636 RNA-Seq. *Bioinformatics* 25, 1105-1111.
- 637 Tang, H.B., Krishnakumar, V., Li, J.P., MichelMoser, Maria, and Cheol Yim W. (2017). Jcvi
638 v0.7.5: JCVI utility libraries. Zenodo. doi:10.5281/zenodo.31631.
- 639 Ueno, K, and Takai, A. (2008). Multiple sex chromosome system of $X_1X_1X_2X_2/X_1X_2Y$ type in
640 lutjanid fish, *Lutjanus quinquelineatus* (Perciformes). *Genetica* 132, 35-41.
- 641 Uyeno, T., and Miller, R.R. (1971). Multiple sex chromosomes in a Mexican Cyprinodontid fish.
642 *Nature* 231, 452-453.
- 643 Uyeno, T., and Miller, R.R. (1971). Multiple sex chromosomes in a Mexican cyprinodontid fish.
644 *Nature* 231, 452-453.
- 645 Walker, B., Abeel, T., Shea, T., Priest, M., Abouelliel, A., Sakthikumar, S., Cuomo, C.A., Zeng,
646 Q.D., Wortman, J., Yong, S.K., et al. (2014). Pilon: An integrated tool for comprehensive
647 microbial variant detection and genome assembly improvement. *PLOS one* 9, e112963.
- 648 White, M.J.D. (1983). *Animal Cytology and Evolution*. Cambridge University Press, Cambridge.
- 649 Xiao, Y.S., Li, J., Ren, G.J., Ma, G.Y., Wang, Y.F., Xiao, Z.Z., and Xu, S.H. (2016). Pronounced
650 population genetic differentiation in the rock bream *Oplegnathus fasciatus* inferred from
651 mitochondrial DNA sequences. *Mitochondrial DNA A* 27, 2045–2052.
- 652 Xiao, Y.S., Xiao, Z.Z., Ma, D.Y., Liu, J. and Li, J. (2019). Genome sequence of the barred
653 knifejaw *Oplegnathus fasciatus* (Temminck & Schlegel, 1884): the first chromosome-level draft
654 genome in the family Oplegnathidae. *GigaScience* 8, giz013.
- 655 Xiao, Z.Z. (2015). Study on population genetics and culture biology of *Oplegnathus fasciatus*.
656 Doctor thesis. P, 162-176.
- 657 Xu, D.D., Sember, A., Zhu, Q.H., de Oliveira E.A., Liehr, T., Al-Rikabi A.B.H., Xiao, Z.Z., Song,

- 658 H.B., and de Bello Cioffi, M. (2019). Deciphering the Origin and Evolution of the X₁X₂Y System
659 in Two Closely-Related *Oplegnathus* Species (Oplegnathidae and Centrarchiformes). *Int. J. Mol.*
660 *Sci.* *20*, 3571
- 661 Xu, D.D., You, F., Lou, B., Geng, Z., Li, J., and Xiao, Z.Z. (2012). Comparative analysis of
662 karyotype and C-banding in male and female *Oplegnathus fasciatus*. *Acta Hydrobiol. Sin.* *36*,
663 552-557.
- 664 Xue, R., An, H., Liu, Q.H., Xiao, Z.Z., Wang, Y.F., and Li, J. (2016). Karyotype and Ag-NORs in
665 male and female of *Oplegnathus punctatus*. *Oceanol. Limnol. Sin.* *47*, 626-632.
- 666 Yang, X.F., Liu, H.P., Ma, Z.H., Zou, Y., Zou, M., Mao, Y.Z., Li, X.M., Wang, H., Chen, T.S., and
667 Wang, W.M. (2018). Chromosome-level genome assembly of *Triplophysa tibetana*, a fish adapted
668 to the harsh high-altitude environment of the Tibetan Plateau. *Mol. Ecol. Resour.* *19*, 1027-1036.
- 669 Yang, Z.H. (2007). PAML 4: Phylogenetic Analysis by Maximum Likelihood. *Mol. Biol. Evol.* *24*,
670 1586-1591.
- 671 Zhang, B.C., Zhang, J., Xiao, Z.Z. and Sun, L. (2014). Rock bream (*Oplegnathus fasciatus*)
672 viperin is a virus-responsive protein that modulates innate immunity and promotes resistance
673 against megalocytivirus infection. *Dev. Comp. Immunol.* *45*, 35-42.
- 674 Zhang, S., Zheng, J., Zhang, J., Wang, Z.Y., Wang, Y., and Cai, M. (2018). Cytogenetic
675 characterization and description of an X₁X₁X₂X₂/X₁X₂Y sex chromosome system in *Collichthys*
676 *lucidus* (Richardson, 1844). *Acta Oceanol. Sin.* *37*, 34-39.
- 677 Zheng, Q.Y. (2019). The role of 11 β -hydroxylase (Cyp11b2) on gametogenesis in tilapia. Master
678 dissertation. P, 10-30.

Table 1. Summary of male *O. fasciatus* genome assembly and annotation

Genome assembly			
	Draft scaffolds for male <i>O. fasciatus</i>	Chromosome-length scaffolds based on Hi-C for male <i>O. fasciatus</i>	**Chromosome-length scaffolds based on Hi-C for female <i>O. fasciatus</i>
Length of genome (bp)	795,074,755	762,267,613	768,808,243
Number of contigs	2,295	1,355	1,372
Contigs N50 (bp)	2,127,178	2,183,645	2,130,780
Number of scaffold	/	23	24
Scaffold N50 (bp)	/	32,431,321	33,548,962
Genome coverage (X)	251.1		314.6
Number of contigs (\geq 100 kb)	881	891	708
Total length of contigs (\geq 100 kb)	736,155,642	733,715,954	732,827,446
Mapping rate of contigs (\geq 100 kb) (%)	/	99.67	99.67
Genome annotation			
Protein-coding gene number	24,835		24,003
Mean transcript length (kb)	15.8		16.1
Mean exons per gene	10.0		10.1
Mean exon length (bp)	220.1		217.7
Mean intron length (bp)	1,511.7		1527.4

** The data was cited from the reference (Yongshuang Xiao, Zhizhong Xiao, Daoyuan Ma, Jing Liu, Jun Li. Genome sequence of the barred knifejaw *Oplegnathus fasciatus* (Temminck & Schlegel, 1844): the first chromosome-level draft genome in the family Oplegnathidae, GigaScience, Volume 8, Issue 3, March 2019, giz013, doi.org/10.1093/gigascience/giz013)

Table 2. Genome quality of *O. fasciatus* based on the BUSCO assessment

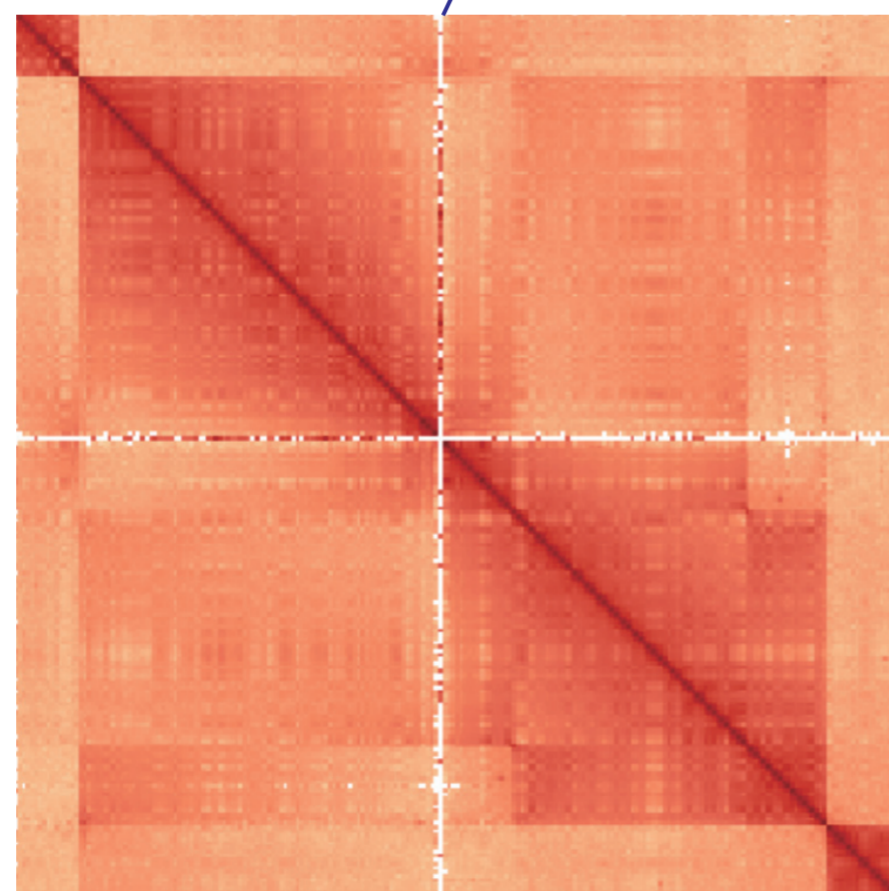
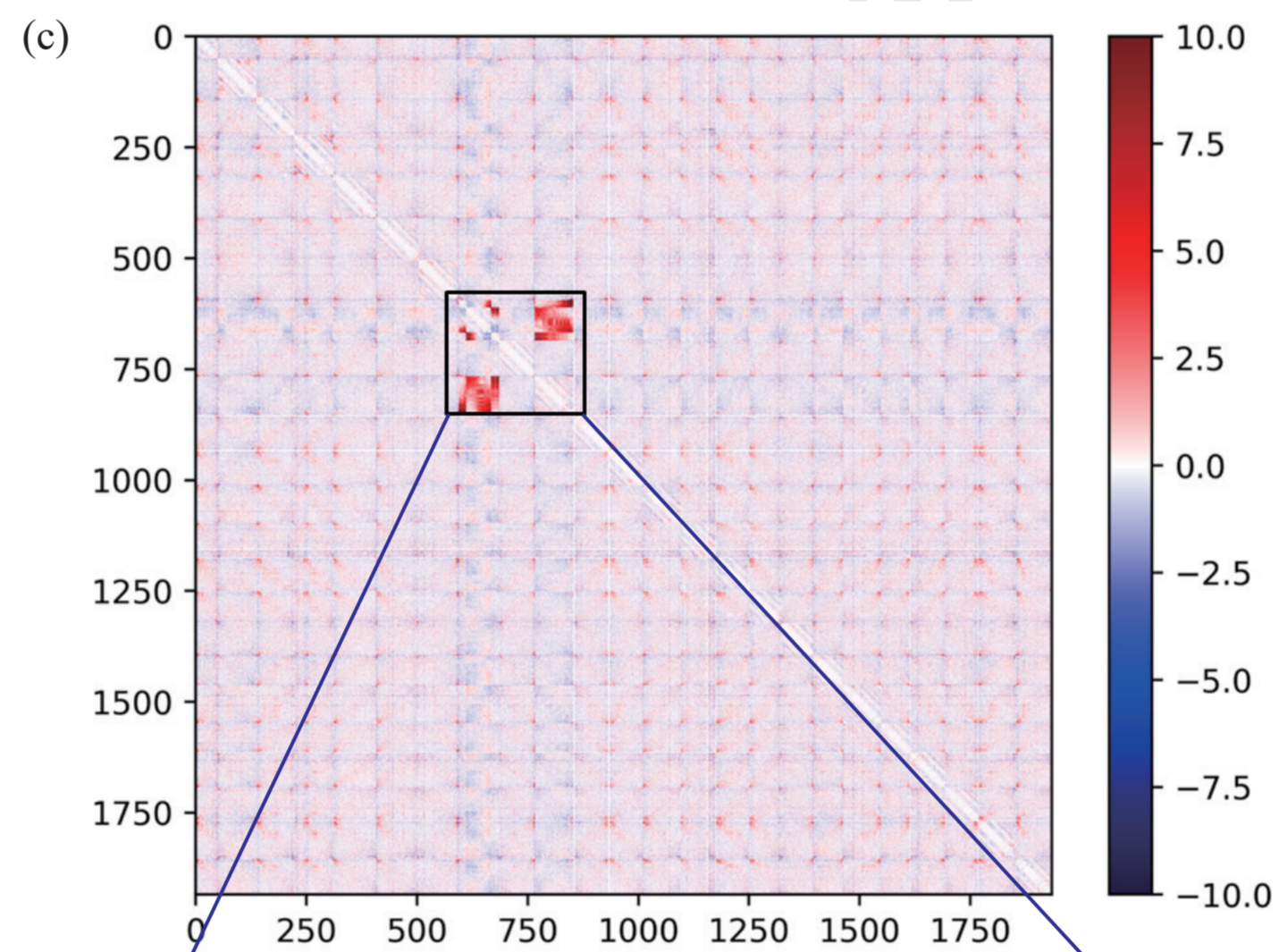
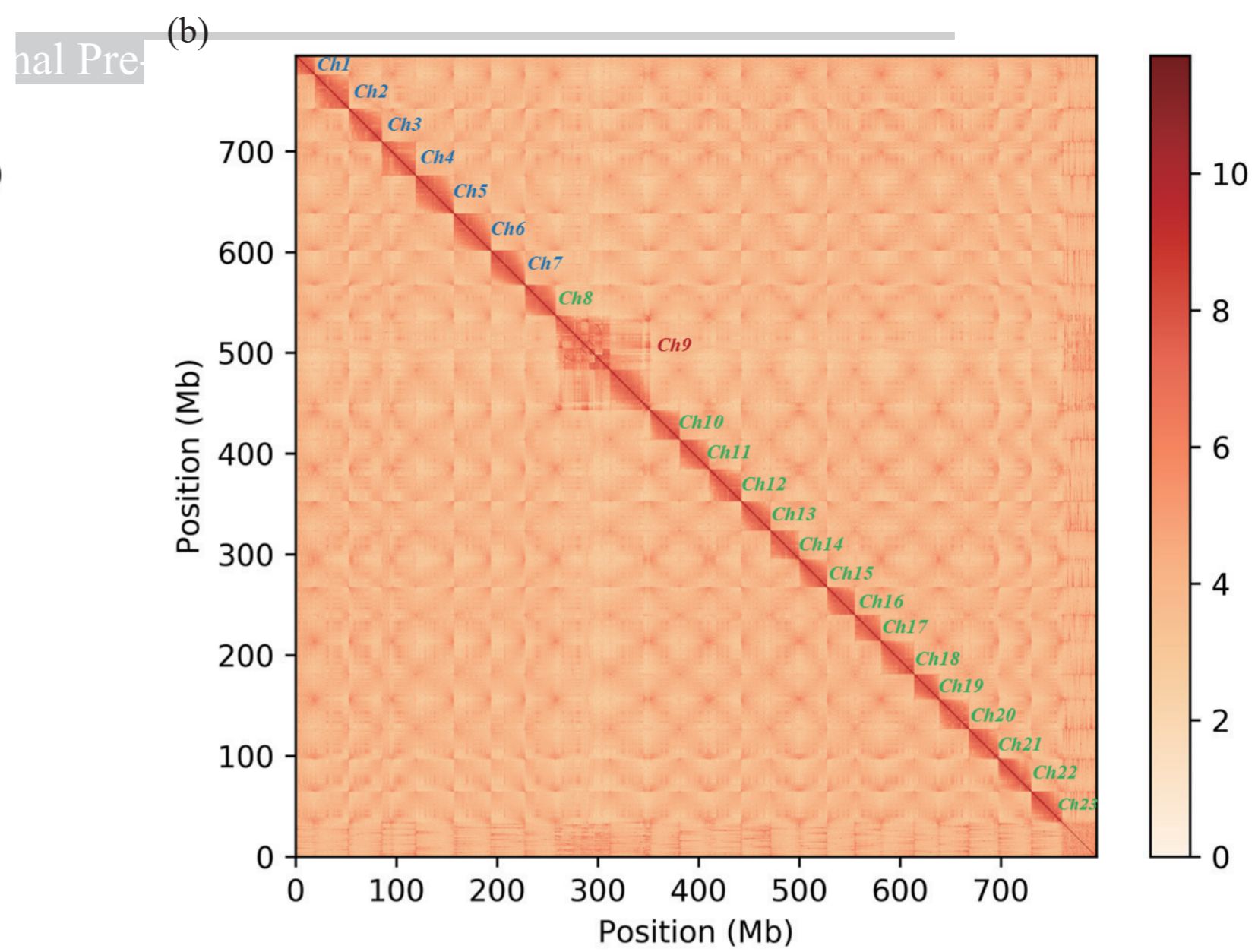
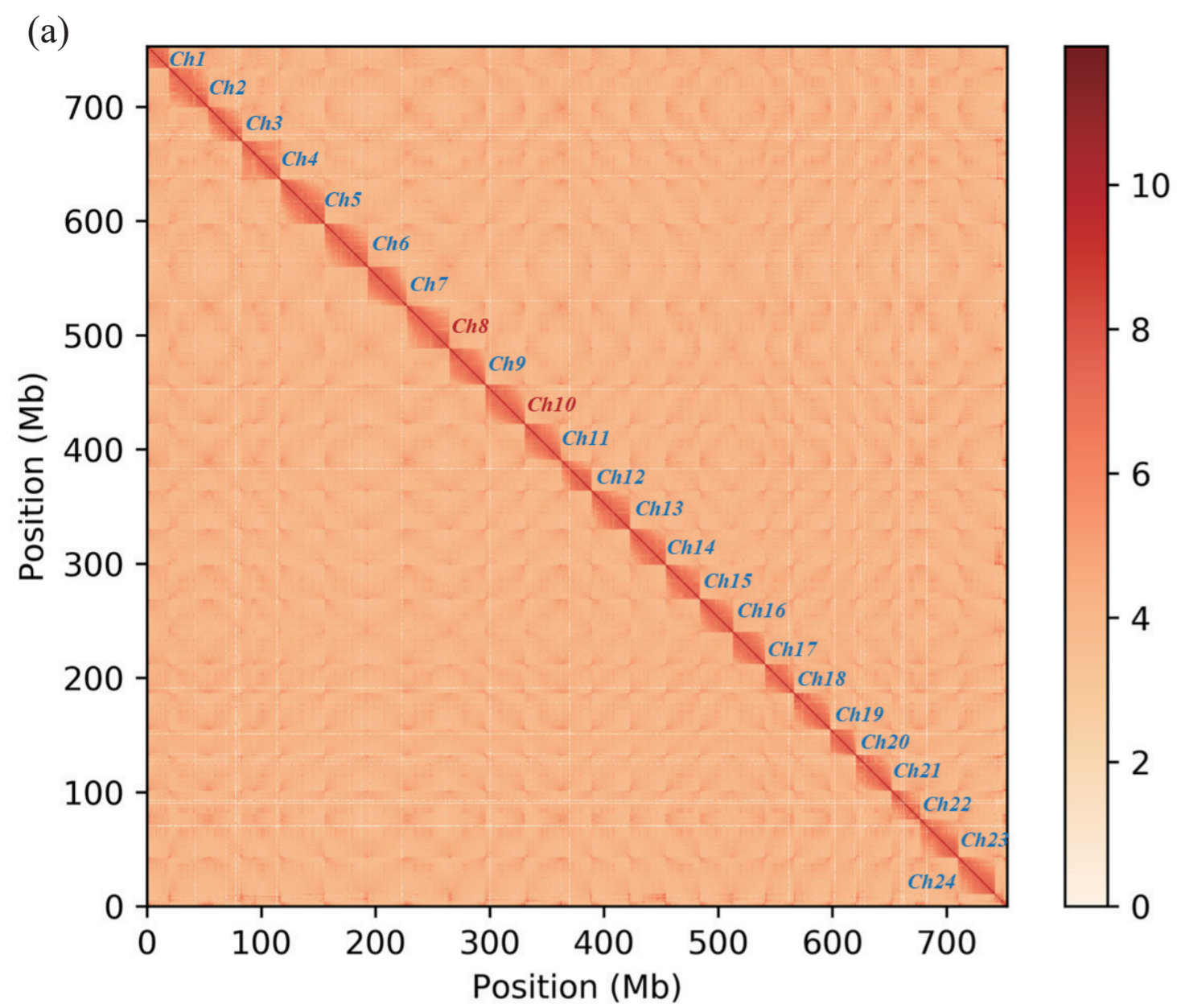
Type	Assembly		Annotation	
	Proteins	Percentage (%)	Proteins	Percentage (%)
Complete BUSCOs	4,456	97.2	4,435	96.8
Complete and single-copy BUSCOs	4,210	91.8	4,143	90.4
Complete and duplicated BUSCOs	246	5.4	292	6.4
Fragmented BUSCOs	48	1.0	66	1.4
Missing BUSCOs	80	1.8	83	1.8
Total BUSCOs groups searched	4,584	100.0	4,584	100.0

Table 3. The detailed classification of repeat sequences for male *O. fasciatus*

Type	Rebase TEs		TE proteins		De novo		Combined TEs	
	Length (bp)	% in genome	Length (bp)	% in genome	Length (bp)	% in genome	Length (bp)	% in genome
DNA	39,085,328	4.92	5,858,619	0.74	83,843,085	10.55	115,535,672	14.53
LINE	24,759,524	3.11	17,460,721	2.20	56,286,293	7.08	85,210,163	10.72
SINE	889,332	0.11	0	0.00	1,986,947	0.25	2,817,685	0.35
LTR	10,536,213	1.33	6,615,817	0.83	32,670,415	4.11	44,682,943	5.62
Satellite	1,910,832	0.24	0	0.00	733,763	0.09	2,480,580	0.31
Simple_repeat	1,304,732	0.16	0	0.00	7,478,505	0.94	8,578,237	1.08
Other	6,957	0.00	171	0.00	0	0.00	7,128	0.00
Unknown	338,847	0.04	0	0.00	30,384,129	3.82	30,719,924	3.86
Total	74,440,379	9.36	29,922,429	3.76	184,141,930	23.16	252,879,666	31.81

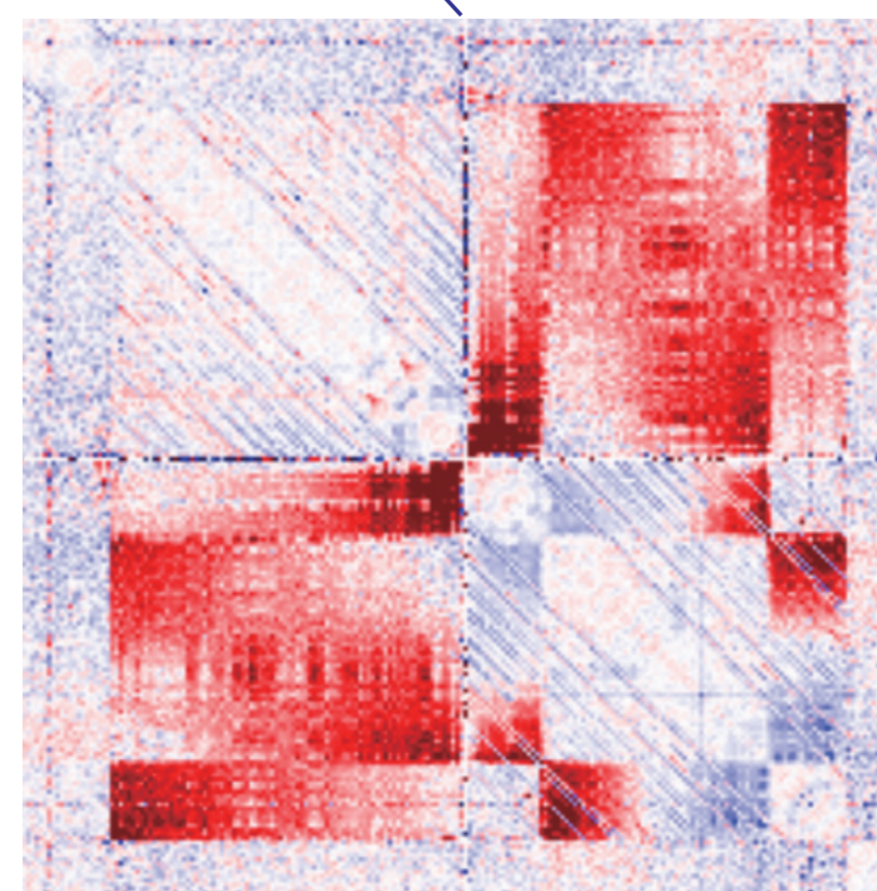
Table 4. Functional annotation of the protein-coding genes in male *O. fasciatus* genome

Type		Number	Percent (%)
Total		24,835	
Annotated	InterPro	21,696	87.36
	GO	16,494	66.41
	KEGG_ALL	23,916	96.30
	KEGG_KO	15,260	61.45
	Swissprot	22,380	90.11
	TrEMBL	23,953	96.45
	NR	24,072	96.93
Annotated		24,105	97.06
Unannotated		730	2.94



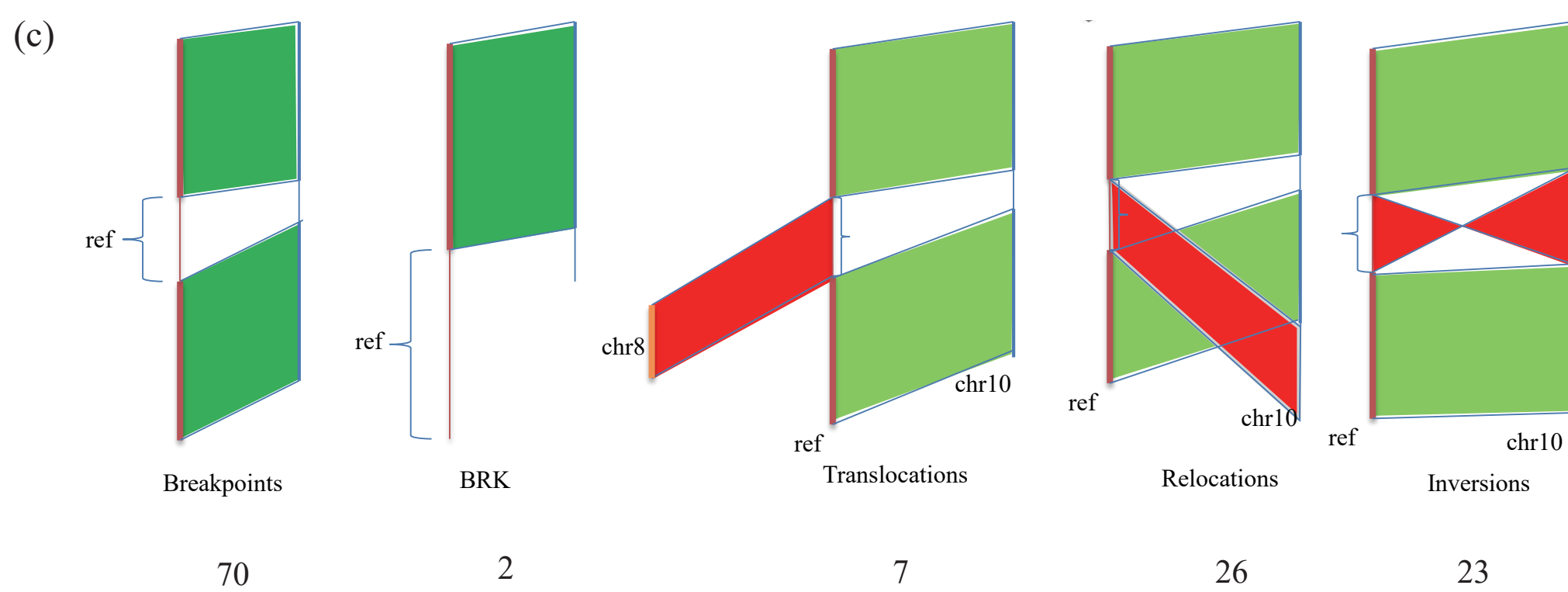
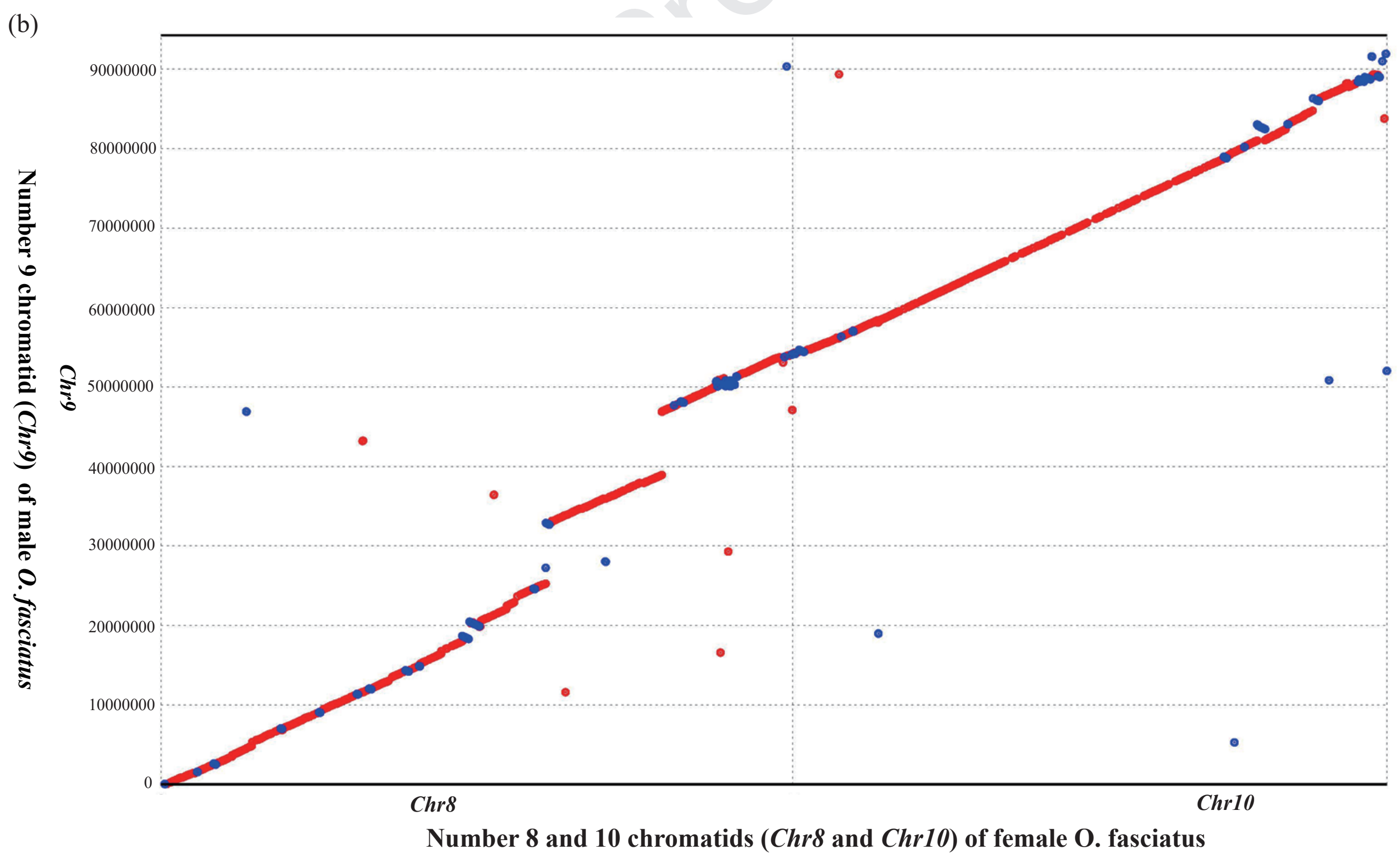
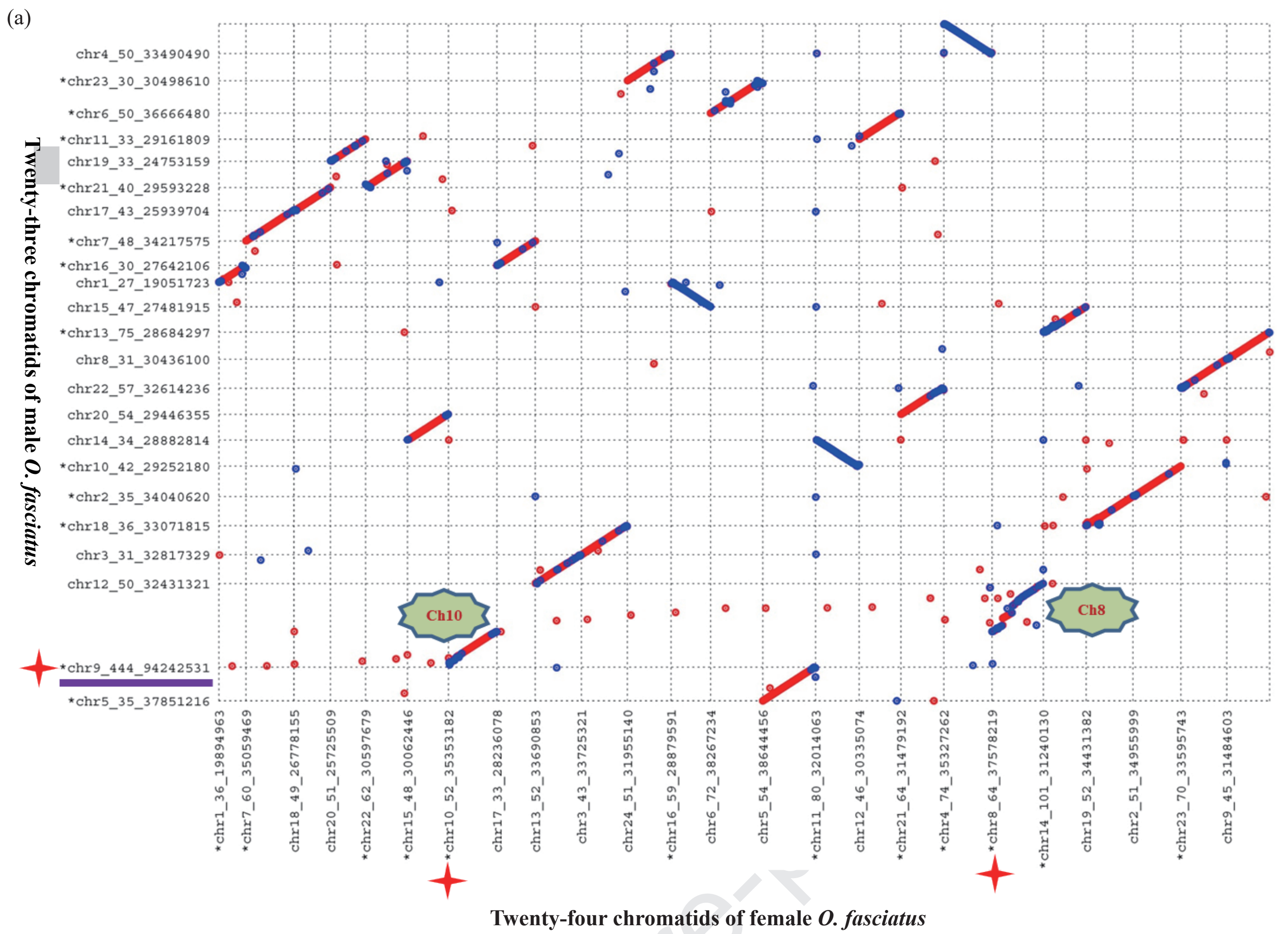
The district corresponding to the number 10 chromatid of female *O. fasciatus*

The district corresponding to the number 8 chromatid of female *O. fasciatus*

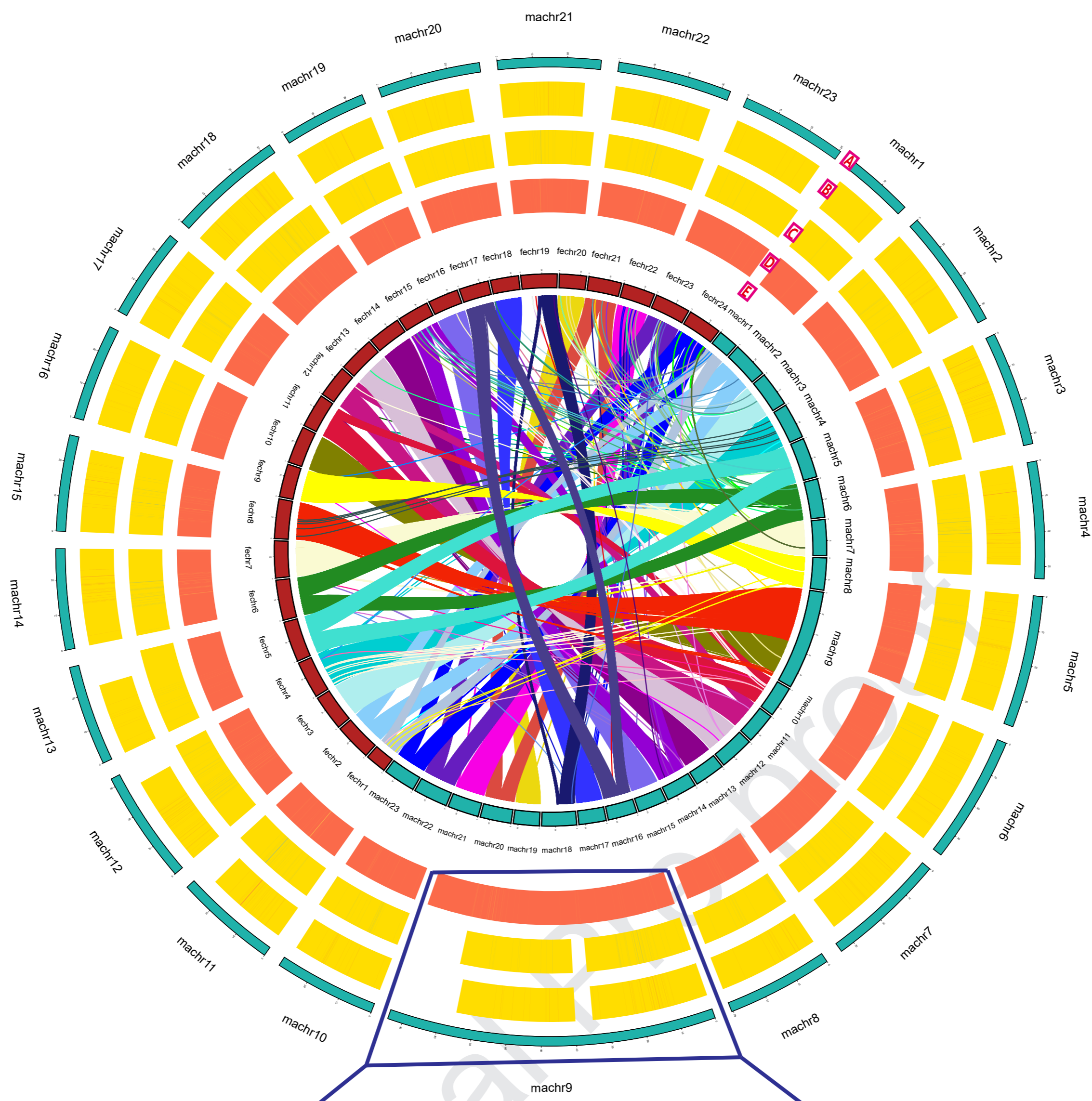


Neo-Y corresponding to the number 9 chromatid of male *O. fasciatus*

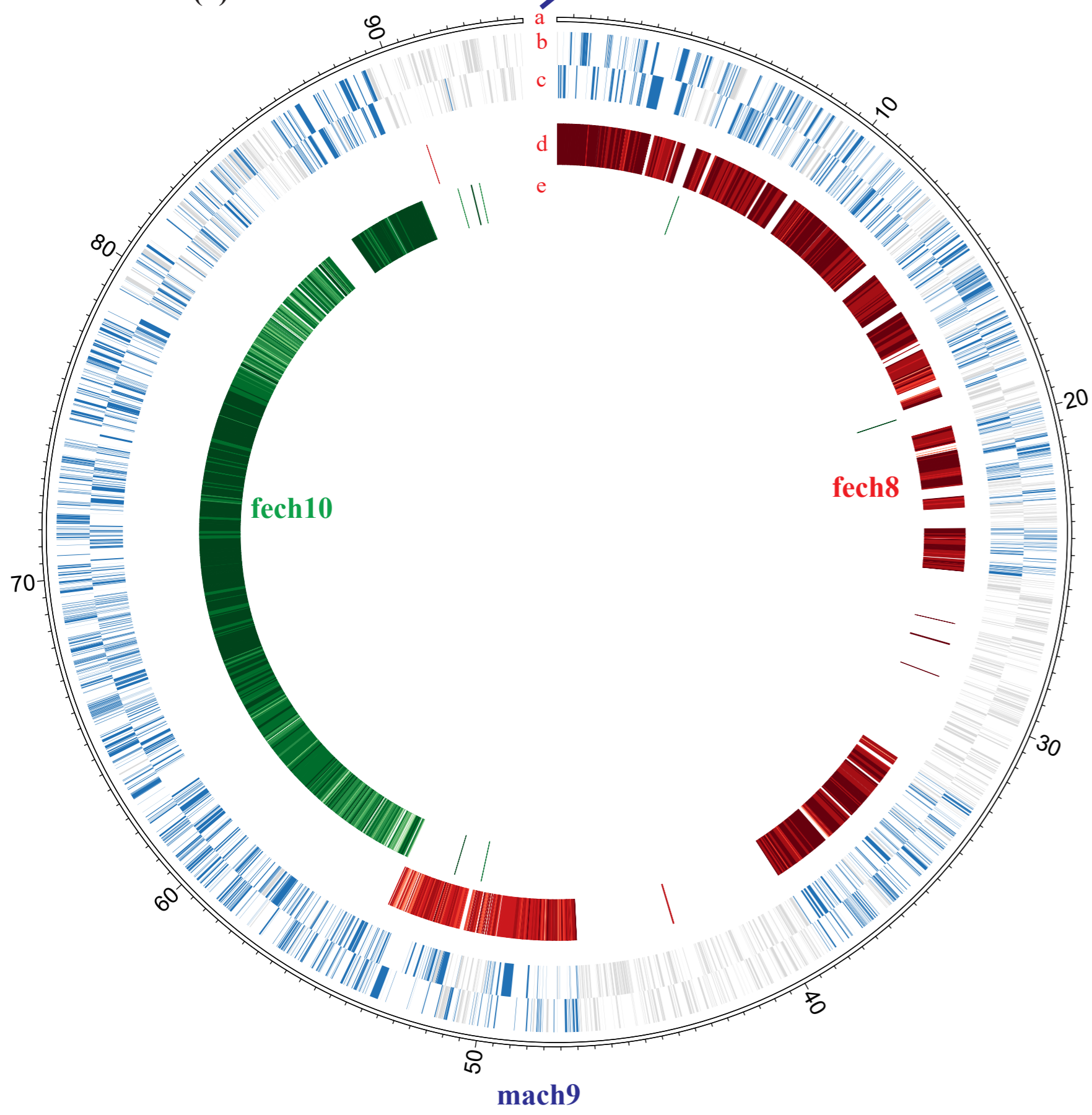
fasciatus



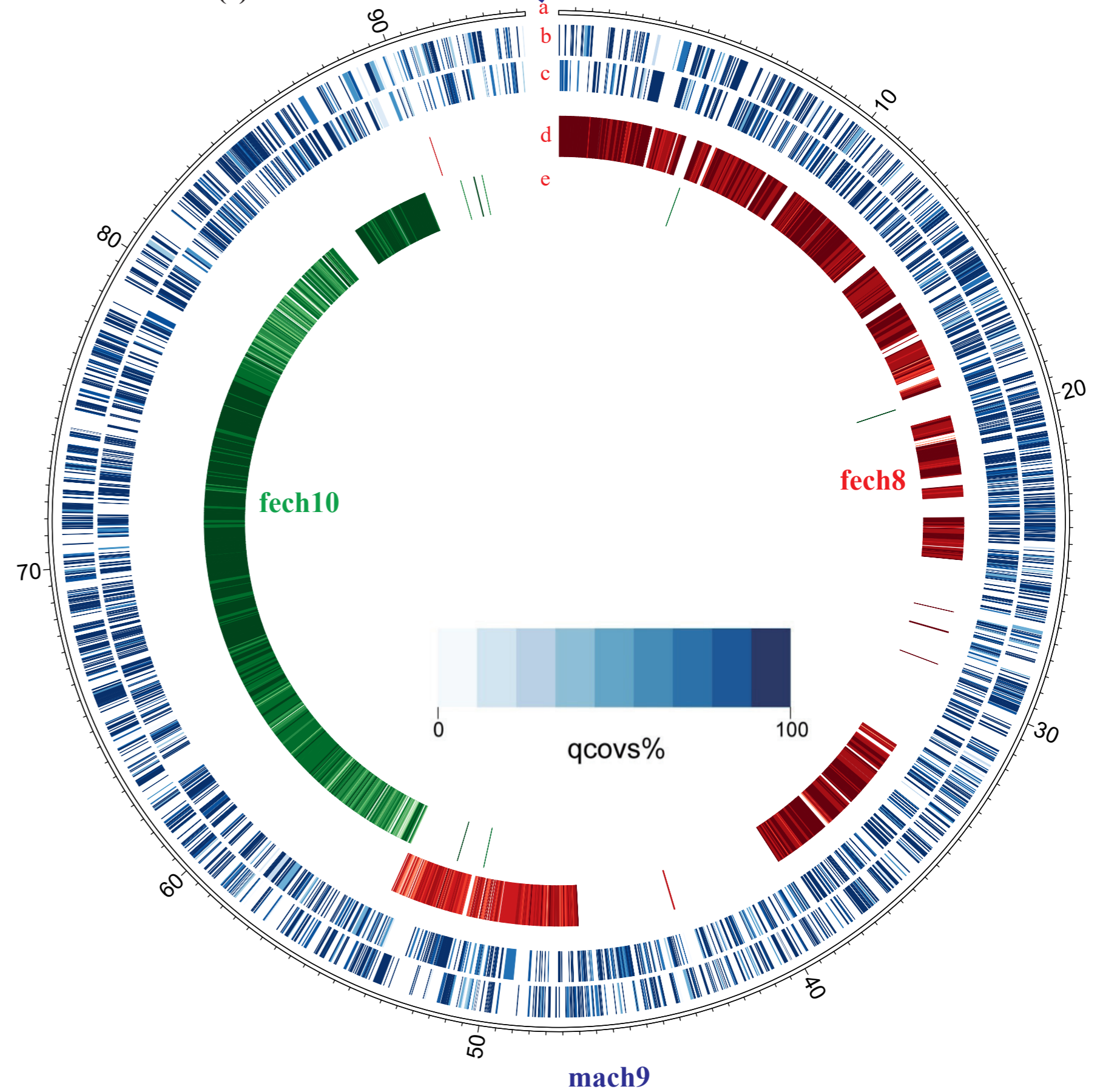
(a)



(b)



(c)



Medaka

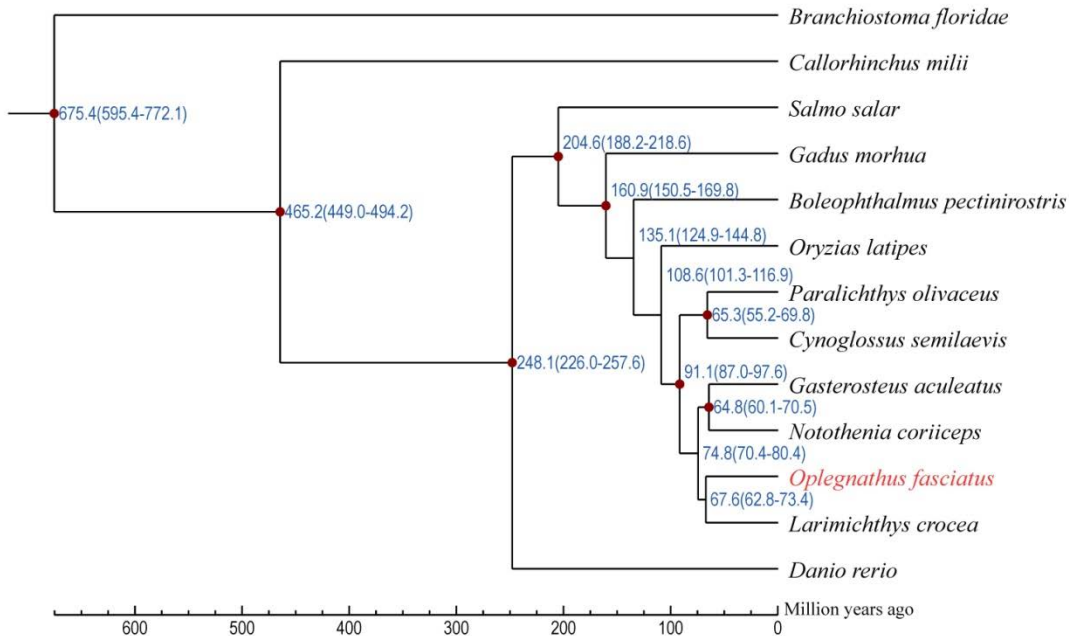


Barred knifejaw male



Barred knifejaw female





Chromosome-level Genome Reveals the Origin of Neo-Y Chromosome in the Male Barred knifejaw *Oplegnathus fasciatus*

Yongshuang Xiao, Zhizhong Xiao, Daoyuan Ma, Chenxi Zhao, Lin Liu, Hao Wu,

Wenchao Nie, Shijun Xiao, Jing Liu, Jun Li, Angel Herrera-Ulloa

HIGHLIGHTS

- 1、 Construction of a chromosome-level reference genome for the male *O. fasciatus*
- 2、 Identification of the origin of neo-Y chromosome to the X_1X_2Y system
- 3、 Accurate comparisons of sequences and genes between female $X_1X_1X_2X_2$ and male X_1X_2Y